

Auditory Motion Induces Directionally Dependent Receptive Field Shifts in Inferior Colliculus Neurons

WILLARD W. WILSON¹ AND WILLIAM E. O'NEILL^{1,2}

¹Program in Neuroscience and ²Department of Physiology, University of Rochester School of Medicine and Dentistry, Rochester, New York 14642

Wilson, Willard W. and William E. O'Neill. Auditory motion induces directionally dependent receptive field shifts in inferior colliculus neurons. *J. Neurophysiol.* 79: 2040–2062, 1998. This research focused on the response of neurons in the inferior colliculus of the unanesthetized mustached bat, *Pteronotus parnellii*, to apparent auditory motion. We produced the apparent motion stimulus by broadcasting pure-tone bursts sequentially from an array of loudspeakers along horizontal, vertical, or oblique trajectories in the frontal hemifield. Motion direction had an effect on the response of 65% of the units sampled. In these cells, motion in opposite directions produced shifts in receptive field locations, differences in response magnitude, or a combination of the two effects. Receptive fields typically were shifted opposite the direction of motion (i.e., units showed a greater response to moving sounds entering the receptive field than exiting) and shifts were obtained to horizontal, vertical, and oblique motion orientations. Response latency also shifted as a function of motion direction, and stimulus locations eliciting greater spike counts also exhibited the shortest neural latency. Motion crossing the receptive field boundaries appeared to be both necessary and sufficient to produce receptive field shifts. Decreasing the silent interval between successive stimuli in the apparent motion sequence increased both the probability of obtaining a directional effect and the magnitude of receptive field shifts. We suggest that the observed directional effects might be explained by “spatial masking,” where the response of auditory neurons after stimulation from particularly effective locations in space would be diminished. The shift in auditory receptive fields would be expected to shift the perceived location of a moving sound and may explain shifts in localization of moving sources observed in psychophysical studies. Shifts in perceived target location caused by auditory motion might be exploited by auditory predators such as *Pteronotus* in a predictive tracking strategy to capture moving insect prey.

INTRODUCTION

We report here on the neurophysiological response to simulated auditory motion. Our fundamental questions were whether motion might affect the spatial processing of a sound and whether specialization for acoustical features specific to motion exists in the auditory domain. On a behavioral level, auditory motion processing is important for determining spatial information in the presence of sound source and/or listener movement. Accurate auditory spatial processing is particularly important for the survival of auditory predators, such as insectivorous bats. Microchiropteran bats emit high-frequency echolocation pulses and rely on information in the returning echoes for obstacle avoidance as well as for prey detection, tracking, and capture (Griffin 1958). The acoustical image of the environment changes

as bats approach stationary objects reflecting their biosonar emissions, producing an “acoustical flow field” (Lee et al. 1992). In addition, both the bat and its prey are typically in flight, and intricate paths of motion from prey echoes also may be produced. Auditory spatial processing therefore must be carried out in a continuously changing acoustic environment, and echolocating bats should rely very heavily on auditory motion processing to track and capture insects on the wing.

In comparison with visual motion, the encoding of auditory motion is problematic. Visual spatial processing is inherent in the optics and retinal organization of the eye, which preserve the spatial characteristics of a stimulus. This spatial information is maintained in place-coded activity maps throughout the retinotopically organized central visual pathway. Such maps are thought to convey the state of that mapped feature (e.g., visual location) and to facilitate higher-order feature extraction based on the mapped stimulus parameter (Knudsen et al. 1987). Higher-order specialization for motion processing is well documented in the visual system. In primate visual cortex, for example, cells that respond well to motion in one preferred direction and poorly in other “null” directions are thought to encode motion direction (e.g., Albright et al. 1984; Baker et al. 1981; Felleman and Kaas 1984; Maunsell and Van Essen 1983; Mikami et al. 1986) and target motion features are carried by neurons in a specialized “motion pathway” (Van Essen and Maunsell 1983).

By contrast to retinotopic maps of visual space, central auditory nuclei preserve cochleotopic maps of stimulus frequency. The location of an auditory stimulus is not readily available from such maps and therefore must be calculated from differences in stimulus timing or intensity between the ears. Because information about location is produced by different mechanisms in the visual and auditory systems, the basis for motion processing also would be expected to differ in the two modalities. We sought to compare motion processing in the auditory modality to its visual counterpart and to explore how the calculation of auditory space is influenced by changing the acoustic variables in the midst of those calculations.

Earlier studies have demonstrated an influence of motion direction on the responses to moving sounds using both real and apparent motion stimuli (e.g., Ahissar et al. 1992; Kleiser and Schuller 1995; Rauschecker and Harris 1989; Spitzer and Semple 1991, 1993; Stumpf et al. 1992; Takahashi and Keller 1992; Toronchuk et al. 1992; Wagner and

Takahashi 1990, 1992; Yin and Kuwada 1983). While motion, direction and/or velocity were shown to influence the response to sound in these studies, the exact nature of motion sensitivity and the mechanisms producing this sensitivity are not yet fully characterized. The present study is a large-scale examination of free-field apparent motion responses in an unanesthetized mammalian preparation, explores such factors as motion velocity and orientation, and includes vertical and oblique motion orientations.

The subject of this study, Parnell's mustached bat (*Pteronotus parnelli*), has been particularly well studied with regard to the cellular mechanisms of stationary sound localization. *Pteronotus* acoustically scans its environment with "long CF/FM" sonar pulses, consisting of a long constant-frequency portion, followed by a short, downward-sweeping, frequency modulation (Novick 1963a). As in other echolocating bats (Griffin et al. 1960), the acoustic behavior of *Pteronotus* follows a stereotypical pattern during approach to a target that can be divided into search, approach, and terminal phases (Novick 1963b). Sonar pulse duration progressively decreases from a maximum of ~30 ms during the initial search phase to a minimum of ~6 ms immediately before contact (Novick and Vaisnys 1964). Similarly, the interval between successive pulses decreases from ~200 ms during the search phase to ~10 ms in the terminal phase (Novick 1963b). Thus information about the environment is gathered as a series of "acoustic snapshots," and the rate at which these snapshots are updated varies with distance to target.

The *Pteronotus* biosonar signal contains five harmonics, but the second, at ~60 kHz, is most prominent (Gooler and O'Neill 1987; Novick 1963a). The primary auditory pathway demonstrates sharp tuning and an overrepresentation of the second harmonic (Henson 1973; Kössl and Vater 1985; O'Neill 1985; Pollak et al. 1972; Ross et al. 1988; Suga and Jen 1976; Suga and Manabe 1982; Suga et al. 1975; Zook et al. 1985). About one-third of the central nucleus (ICC) of the inferior colliculus (IC) is devoted to representation of the 60-kHz harmonic, and cells tuned to that frequency range have low thresholds and are tuned extremely sharply (Grinnell 1970; O'Neill 1985; Pollak and Bodenhamer 1981). These units are clustered into the cytoarchitecturally distinct dorsoposterior division (DPD) (O'Neill et al. 1989; Pollak and Bodenhamer 1981; Zook et al. 1985), which can be considered an enormously hypertrophied isofrequency lamina (Zook et al. 1985). The DPD therefore provides a unique view into the functional organization for auditory spatial processing within a single isofrequency lamina. For example, Wenstrup et al. (1986) have demonstrated an intralaminar organization of binaural response types within the DPD and have described a map of sensitivity to interaural intensity difference (IID) with depth in the "EI area" of the DPD. However, echolocating bats are capable of both active and passive sound localization (e.g., Faure and Barclay 1992; Fuzessery et al. 1993; Kanwal et al. 1994), and there is no evidence to suggest that active and passive localization in azimuth and elevation are subserved by different neural mechanisms or structures (Fuzessery and Pollak 1985; Hutson and Kieber 1997; Pollak et al. 1995; Zook and Casseday 1982a,b). The neural processing of azimuth and elevation by echolocating bats there-

fore can be considered to follow the general mammalian plan.

In this study, sensitivity to free-field apparent motion was tested in the DPD, a neural substrate functionally organized for the processing of auditory space (Wenstrup et al. 1986). Apparent motion was produced by jumping a tone burst across an array of speakers in lieu of actual motion of a single speaker. In psychoacoustical experiments, this form of apparent motion gives rise to perceptions akin to real motion (Burt 1917; Strybel et al. 1989, 1992) and has the advantage of producing none of the extraneous noise associated with a mechanically moving sound source (e.g., motors, bearings, wind noise, etc.). It also has the advantage that it approximates the acoustic stimulation normally experienced by echolocating bats, which emit temporally discrete sonar pulses and thereby experience the world "stroboscopically." This research was designed to characterize further the neural response to auditory motion, to determine relevant stimulus parameters producing a motion response, and to elucidate possible mechanisms giving rise to motion selectivity.

This work represents a portion of the dissertation by W. W. Wilson that was performed in partial fulfillment of the requirements for the PhD degree in the neuroscience program at the University of Rochester.

METHODS

Preparation

Six Jamaican Parnell's mustached bats (*Pteronotus parnelli parnelli*; Chiroptera: Mormoopidae) served as experimental subjects. The animals were maintained on a diet of fortified mealworms in a temperature- (28°C) and humidity- (85–95%) controlled flight room approximating the colony's home cave. All surgical and recording procedures were approved under the animal care and usage guidelines of the University Committee on Animal Resources and conducted in facilities with programs accredited by the American Association of Laboratory Animal Care.

Surgical procedure

Individual bats were prepared under methoxyflurane (Metofane, Pittman-Moore) anesthesia in sterile conditions. The dorsal surface of the skull was exposed by reflecting the overlying skin and musculature laterally, and a small threaded holding tube was attached to the skull with cyanoacrylate glue and dental acrylic. A sharpened tungsten indifferent electrode (125- μ m diam.) then was inserted through a small hole bored in the skull and glued in place contacting the dura. The preceding procedure did not appreciably affect the normal position or motility of the pinnae.

Bats were allowed to recover from anesthesia overnight before the first recording session. Topical anesthetic [lidocaine hydrochloride (Xylocaine), 2%] was applied to the wound margins throughout sessions as needed. Before recording began, a small hole (~500- μ m square) was cut in the skull to permit insertion of the recording electrode. The IC is readily visible through the thin skull of the bat and placement of the hole over the IC was accomplished visually. The specific target was the DPD of the ICC. Recordings also were carried out in the superior colliculus (SC) of one animal using the standard recording setup described in the following section. In addition, a glass micropipette (8- μ m-tip diam) filled with 10% horseradish peroxidase in 0.05 M tris (hydroxymethyl) amino-methane buffer, 0.5 M KCl, pH 7.6 was used to record activity in the SC and to mark an iontophoretic injection site. Subsequent

histological processing (after Mesulam 1982) was used to verify recording sites.

Recording setup

Experiments were carried out in a shielded, double-walled, temperature-controlled, soundproofed booth (IAC) lined with convoluted foam (Sonex) to attenuate echoes. The awake bat was placed into a form-fitting foam restraint in a custom-built stereotaxic frame (Schuller et al. 1986). The holding tube on the head of the bat then was attached to an arm on the stereotaxic frame such that the head was in a fixed position relative to the loudspeaker array (see further text). Synthetic lamb's wool was draped over the frame to reduce echoes. Only the bat's head, the restraining arm, and a small part of the stereotaxic frame were uncovered and directly in the sound field, and the tube and arm that held the bat's head were never directly between the sound source and the bat's ears. Recording sessions generally lasted 6–8 h per day, and water was provided to the bat at regular intervals during this time.

Parylene-coated tungsten microelectrodes (Micro-Probe) with tip exposures of 10 μm (2.0–2.5 $\text{M}\Omega$ impedance) or glass micropipettes filled with 3 M NaCl or 3 M KCl (impedance $>10 \text{ M}\Omega$) were introduced into the brain with a three-dimensional micromanipulator system and a piezoelectric microdrive (Burleigh Inchworm PZ-555). Neural activity was amplified and recorded with conventional extracellular techniques. Recorded spikes were discriminated from background using a time/amplitude window discriminator (BAK Electronics model DIS-1), and the time of occurrence was recorded by a real-time clock on the laboratory computer (Digital Equipment Corporation Micro PDP 11/23+) in concert with our data acquisition/stimulus presentation package (HAL) written by H. D. Lesser. Additional motion-specific software was written in the C programming language by W. W. Wilson and integrated into the existing package.

Stimulus generation and delivery

Pure tone bursts were the acoustic stimuli used in all experiments. Continuous pure tones were generated by a calibrated function generator (Wavetek Model 111), and tone frequency was monitored by a frequency counter (Optoelectronics FC-50). The signals then were gated into tone bursts with a 1.0-ms linear rise/fall time by an electronic switch (Wilsonics BSIT), sent through a programmable attenuator (Wilsonics PATT), band-pass filtered from 5 to 150 kHz (Krohn-Hite 3202R), and broadcast from a custom-built speaker array. The speaker array's controller board was governed by the computer's parallel I/O port under software control.

The array controller consisted of an extended-bit addressing system and associated multiplexers (used as digital switches). Multiplexers were used rather than relay switches to avoid audible switching transients. The extended-bit addressing hardware used input from the computer's parallel I/O board to activate a selected multiplexer line. Each multiplexer line fed one of 130 possible speakers in the array, and only one speaker was activated at any given time. Controller switching was coordinated with stimulus presentation and data acquisition by the software, and a selected line became active $\geq 25 \text{ ms}$ before a tone burst was passed through it. The tone burst was routed through the active line, biased at 200 V DC and broadcast from that line's corresponding speaker in the array.

The speaker array consisted of 130 electrostatic transducers (Polaroid model T2004-C; 3.8-cm diam, 4.2° subtended angle) mounted on a frame of 10 horizontal semicircular perimeters (51.5 cm radii; Fig. 1). The speakers were mounted symmetrically about midline at 10° intervals on each perimeter, and the perimeters were separated by 10° elevation, forming a $10 \times 10^\circ$ grid that spanned

a 90° range in elevation and a 120° range in azimuth. At the focus of the array, the speaker-to-speaker variation was $\pm 2.05 \text{ dB}$ at 60 kHz measured by a calibrated 1/4-in. microphone (Brüel and Kjaer model 4135) connected to a measuring amplifier (Brüel and Kjaer model 2610). With this setup, tone bursts could be presented either in succession from a single speaker (stationary stimulus) or jumping sequentially from speaker to speaker (free-field apparent motion or FFM).

Pinna movements in response to auditory motion might have confounded the interpretation of our results. However, we observed no pinna movement correlated with stimulus location either by direct visual examination or by examination of video recordings. Furthermore, we have obtained results similar to those reported here for apparent motion stimuli (dynamic IID and dynamic intensity stimuli) presented either through earphones or from a single loudspeaker in the free-field, i.e., conditions unaffected by pinna movements (Wilson and O'Neill 1995).

Experimental procedure

During recording sessions, the intersection of the bat's interaural axis and midline was placed at the focal point of the speaker array. The bat then was positioned such that the lower jaw and interaural axis were aligned with the horizontal axis of the speaker array. This is roughly equivalent to the plane used in other studies of this species (Fuzessery and Pollak 1985; Fuzessery et al. 1992; Makous and O'Neill 1986). The azimuth of a given speaker is expressed as degrees lateral from the midsagittal plane in the hemifield contralateral (CL) or ipsilateral (IL) to the recording site. Speakers above the plane of the jawline have a positive elevation (+e), those below, a negative elevation (−e).

To isolate single units, 30-ms stationary tone bursts were presented at a rate of 5/s (200 ms onset interpulse interval, IPI) from the speaker at 30°CL , -10°e . This is roughly the point of greatest pinna amplification for 60 kHz in this species and the center of DPD spatial preference (Fuzessery and Pollak 1985; Makous and O'Neill 1986). Search stimuli were presented as the electrode was advanced until a single unit was isolated. Most units were driven by stimuli from the contralateral hemifield; however, spontaneously active but unresponsive units were tested with stimuli from midline, the ipsilateral hemifield, and with apparent motion stimuli. In initial experiments, we varied the stimulus location, intensity, and frequency to determine the speaker at which the lowest intensity stimulus at any frequency elicited a stimulus-driven response. These parameters were defined respectively as the best location, minimum threshold (MT), and best frequency (BF) of the cell. To collect more motion data before losing a cell, we later defined the best location as 30°CL , -10°e and determined the BF and MT at this location. Because BF and MT measurements depend on the directional properties of the ear (Gooler et al. 1993), a decrease in frequency tuning accuracy may have resulted from using this fixed, but not necessarily optimal position for each unit.

Apparent motion stimuli

A free-field motion stimulus was presented by sequentially changing the source of BF tone bursts from speaker to speaker through one of four possible orientations (horizontal, vertical, right oblique, and left oblique) through the best location (Fig. 1), usually at 10 dB above minimum threshold. A single "sweep" of motion typically consisted of one round-trip sequence of stimuli moving between the ends of the array, and a single "trial" of motion consisted of 20 sweeps repeated seamlessly. For any motion orientation, the direction that the stimulus moved on the first half-sweep presented was arbitrarily defined as the "forward" direction of motion. At the ends of the array, stimuli were presented twice from the same speaker so that an equal number of stimuli occurred

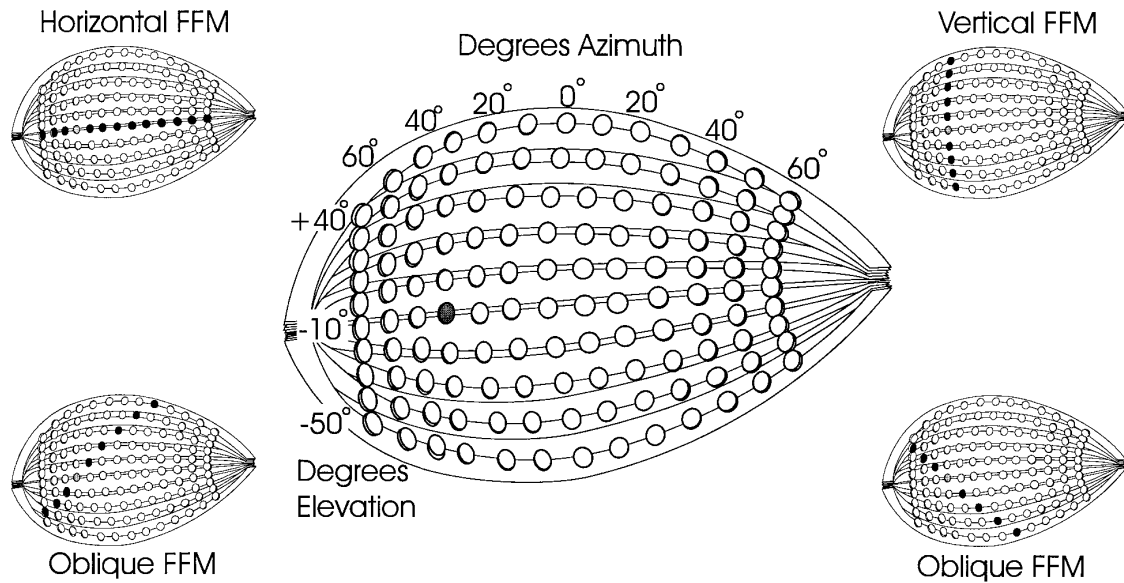


FIG. 1. Free-field stimulus array viewed from the front and slightly to the left. A total of 130 speakers formed a $10 \times 10^\circ$ grid in front of the animal at a radius of 51.5 cm. During free-field experiments, the point where the bat's interaural axis intersects midline was placed at the focal point of this array. Marked speaker shows the best location of a typical cell in the right inferior colliculus (IC) at 30° contralateral (CL) azimuth, -10° elevation. Free-field apparent motion (FFM) was produced by jumping tone bursts back and forth between the ends of the speaker array in any of the 4 orientations allowing straight line motion through the best location (smaller reproductions).

in both directions of motion. We then could determine the effect of motion direction at any speaker by comparing the response elicited by 20 stimuli in the forward motion sequence to 20 otherwise identical stimuli but in the reverse motion sequence. The continuous round-trip nature of the stimulus was used to preclude any effect of the starting direction in the motion sequence, and our pairwise statistical analyses tested for a consistent directional effect across all sweeps. In addition, the effect of FFM starting direction was tested empirically within single units and did not influence the response to this motion paradigm.

Initial experiments indicated that a greater number of sweeps and a subsequent increase in statistical power were desirable. Due to the inherent possibility of losing the cell before a trial was complete, multiple trials with an equal number of sweeps were run, rather than a single trial with a large number of sweeps. This also allowed for a degree of post hoc analysis of the response variability between trials. We attempted to gather at least three identical trials for each stimulus condition. These trials were pooled into a single motion "set" if this proved statistically valid (see *Statistical techniques*).

The data acquisition software time-stamped each spike arrival with a precision of $10 \mu\text{s}$ and generated on-line peristimulus time histograms (PSTs) of the response. For each stimulus presentation, data acquisition usually began 5 ms before the stimulus began and lasted until after the cell had stopped responding. For each trial, stimulus onset times, spike arrival times, the location of the active speaker at the time each spike occurred, and motion direction were stored in individual computer files for off-line analysis. The effect of IPI, stimulus duration, motion orientation, and/or range of motion was determined in some cells.

The shortest temporal gap between stimuli that we could present was constrained by the data acquisition system to ≥ 25 ms. Standard duration/IPI combinations for apparent motion stimuli were 30s/200 ms, 30s/100 ms, and 30s/66.6 ms, although other combinations were used. This stimulus duration is typical of the initial search phase of the echolocation sequence (Novick and Vaisnys 1964), and the set of standard IPIs normally are experienced by *Pteronotus* during approach to a sonar target (Novick 1963b). In

addition, human subjects can perceive motion from a 50-ms tone burst jumping between speakers over this range of IPIs (Strybel et al. 1989). Thus the temporal features of our apparent motion stimuli were both behaviorally relevant to the mustached bat and good approximations of conditions giving rise to motion percepts in humans.

Apparent angular velocity (v) was calculated as a function of the angular separation between speakers (θ) and the IPI between stimulus onsets ($v = \theta/\text{IPI}$) (Rauschecker and Harris 1989; Wagner and Takahashi 1990, 1992). Motion in the horizontal and vertical orientations ($\theta = 10^\circ$) for our standard IPIs therefore had angular velocities of $50^\circ/\text{s}$ (200 ms IPIs), $100^\circ/\text{s}$ (100 ms IPIs), and $150^\circ/\text{s}$ (66.6 ms IPIs). Due to the geometry of the speaker array, oblique orientations of motion ($\theta = 14.14^\circ$) had higher apparent velocities of 71, 141, and $212^\circ/\text{s}$ for the same set of IPIs.

Data analysis

On-line displays of the response as a function of stimulus location and motion direction were used to monitor to the effect of motion direction during a recording session. Only stimulus-driven spikes were included in subsequent off-line analyses. Stimulus-driven spikes were defined as those occurring in a temporal "window" for all data gathered under a given constellation of stimulus characteristics (i.e., IPI, duration, intensity, orientation, etc.). Using the window improved the signal/noise ratio and lowered statistical variability by eliminating the influence of spontaneous activity outside the window. The temporal window was obtained by subjectively determining the response onset and offset for all data files with a given stimulus configuration, displayed as PST histograms with $500\text{-}\mu\text{s}$ binwidths. These multiple estimates of response onset and offset then were used to set an overall best window that was applied as a temporal spike arrival time filter for all files with that stimulus configuration. To ensure that all stimulus-driven spikes were included in the analysis, the best window typically started at the earliest estimate of response onset and ended at the latest estimate of response offset. Output files containing the number of spikes in the analysis window for each stimulus presentation were

produced and transferred to a personal computer for further analysis. Most analyses were written in the RPL language using the RS/1 data analysis package (BBN Software Products).

Statistical techniques

A brief description of our statistical analyses appears here. Detailed statistical procedures are included in the APPENDIX.

DATA POOLING. Multiple trials with identical stimulus parameters were run for most units. Although it was advantageous to increase statistical power by pooling identical trials into a single set, blindly pooling dissimilar results would increase statistical variability. Pooling validity was tested using Kruskal-Wallis tests (Sokal and Rohlf 1981) on the spike count distribution at each speaker location for forward sweeps, reverse sweeps, and the difference between the forward and reverse sweeps.

We found that the response across trials was consistent; all replicates could be pooled for 90% of the sets with multiple trials. Boxplots were used to determine the source of any significant difference, and if a trial could not be pooled, it was removed from the set and the remaining trials were tested for pooling validity. The largest statistically valid set was used for all subsequent analyses.

DIFFERENCE IN DISCHARGE MAGNITUDE OR "DIRECTIONAL BIAS." One way that the neural response in the two apparent motion directions might differ was for a greater overall response to occur in one direction of apparent motion over the other (i.e., a directional bias). The Wilcoxon signed-rank test was used to test whether the total number of spikes elicited by the forward sweeps of motion in a set differed from that to the reverse sweeps at a significance level of $P \leq 0.05$ without regard to the particular locations at which this effect may have occurred.

DIRECTIONALLY DEPENDENT SHIFT IN RECEPTIVE FIELD (LINEAR COMBINATION). Another possible effect of apparent motion was a shift in a unit's receptive field location for the forward and reverse directions of motion with or without a coincident directional bias in spike count. We used a custom "linear combination" statistical procedure to determine whether such a shift was significant. The linear combination was designed to detect a shift in the location of the receptive fields in opposite motion directions by testing for a consistent pattern in the difference between them, allowing, but not requiring, the curves to cross at a single point.

The response at a given location, sweep, and direction was normalized to eliminate any response magnitude effect in the linear combination analysis. This was necessary because a directional bias summed over all locations would also produce a consistent pattern in the area between the forward and reverse curves. Because the difference in response magnitude was examined previously with the Wilcoxon test, response magnitude information was blocked out of the linear combination but was not lost. The normalization allowed us to use the linear combination to test for differences in curve *shape*, eliminating the influence of differences in curve *size*.

LATENCY ANALYSIS. For spike latency analysis, the latency of the first spike for each stimulus presentation in a latency analysis window was analyzed. This window was similar to the spike count window except that the PST bin containing the last spike in the *phasic* portion of the response marked the end of the analysis window. This temporal filter prevented a skewed first spike latency distribution because of first spikes in the tonic portion of the response and reduced variability in the distribution by blocking out background activity before the evoked response. Statistical analyses were not performed on the spike latency data because many stimuli (e.g., at locations outside the receptive field) had zero spikes in the phasic response window, severely decreasing the n and invalidating statistical assumptions used in the spike count analysis.

RESULTS

Single-unit recordings for free-field apparent auditory motion were obtained in 92 single units in the IC and 3 single units in the SC. The BFs of the IC units ranged from 60.15 to 63.98 kHz, and their response properties were consistent with the well-documented response properties of DPD neurons (Fuzessery and Pollak 1985; Grinnell 1970; O'Neill 1985; O'Neill et al. 1989; Pollak and Bodenhamer 1981; Zook et al. 1985). Although this range of BFs exceeds that typically found within the DPD of a given bat, it was due primarily to differences between the six bats included in this study, likely reflecting individual differences in their "resting" vocalization frequency and cochlear tuning. Histological processing was used to confirm SC recording sites. The SC units did not have markedly different response properties from IC units and therefore are included in the overall analysis.

All units were responsive to both stationary search stimuli and apparent auditory motion; there were no "motion specialized" neurons in our sample that responded exclusively to apparent motion. This result corroborates the findings in other studies of free-field auditory motion (e.g., Rauschecker and Harris 1989; Wagner and Takahashi 1990, 1992) and is in contrast to directionally selective visual unit, which respond poorly or not at all to stationary stimuli (Albright et al. 1984; Hubel and Weisel 1962; Maunsell and Van Essen 1983).

A significant difference in the response between the two directions of motion (a "directional effect") was observed in 65% ($n = 62$) of the 95 units tested. We could not assess responses to all possible conditions of apparent motion in each of the isolated units, and in many units, the directional response changed depending on the characteristics of the stimulus. However, we found three consistent types of directional effects across units and motion conditions. A directional effect could take the form of a shift in the receptive field location (RF shift), a difference in response magnitude (directional bias), or a combination of the two effects.

Apparent motion produces receptive field shifts

An example of a receptive field shift (RF shift) to horizontal motion is shown in Fig. 2A, *top*. For both directions of motion, this cell responded in a restricted portion of the frontal hemifield, from $\sim 10^\circ$ IL to $\sim 50^\circ$ CL, typical of the contralateral preference generally observed at the level of the IC (see Irvine 1992 for review). There was no directional bias in this unit: the mean response in the two directions of motion was not significantly different. However, although motion did not alter the speaker locations to which the cell responded or the overall firing rate of the cell, the shape of the receptive field clearly changed with motion direction.

Consider the response at 40° CL azimuth to stimuli differing only in apparent motion direction. Motion toward the ipsilateral hemifield elicited ~ 2.7 spikes/stimulus, whereas motion toward the contralateral hemifield elicited only ~ 1.6 spikes/stimulus from this location, a decrease of $\sim 40\%$. Motion also affected the response on the medial receptive field border, but at these locations, the response to ipsilateral motion was lower than contralateral motion. At 0° azimuth, motion toward the contralateral hemifield elicited more than

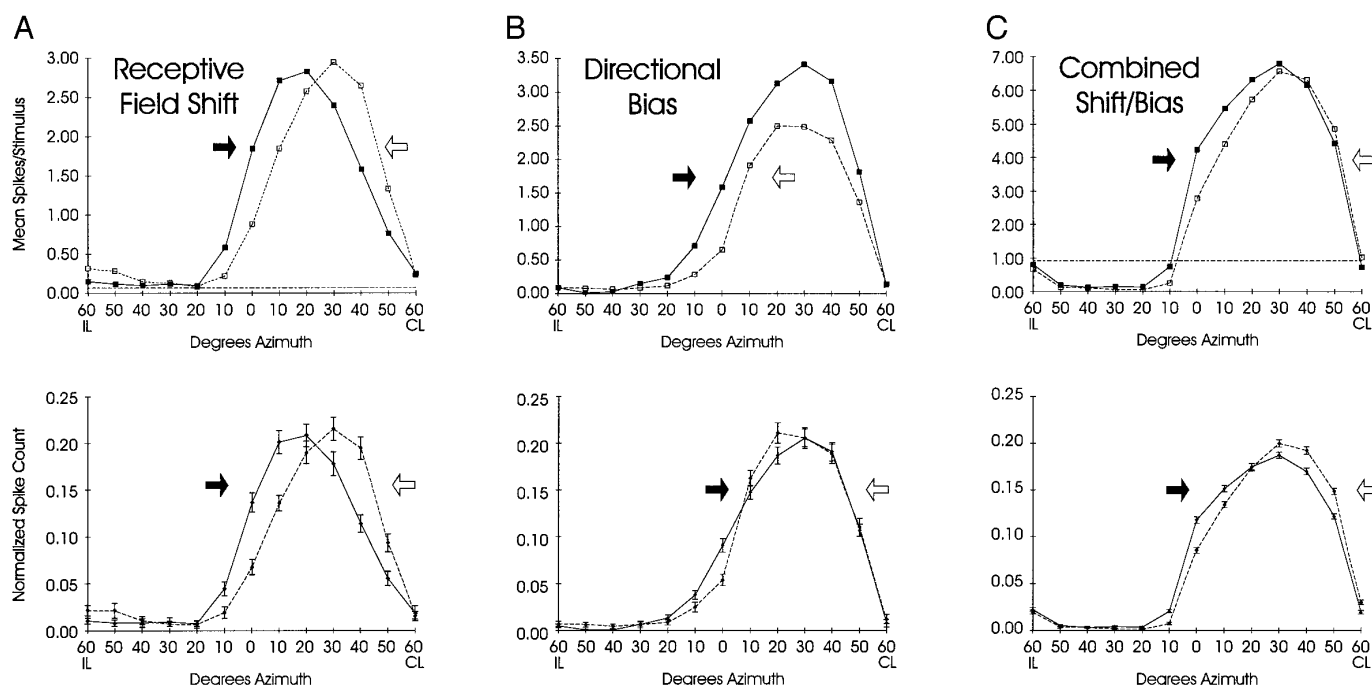


FIG. 2. *Top*: response at each speaker location for opposite horizontal motion directions, averaged across all trials in a pooled FFM set. In this and all subsequent motion graphs, the response to motion from points displayed on the left side of the x axis toward those on the right is shown by the curve with the filled symbols and from the points on the right side toward points on the left by the curve with open symbols. The dashed horizontal line represents the average background firing rate measured with no acoustic stimulus and subjected to the same temporal window as the other data for the set (when available). *Bottom*: same data normalized as described in the APPENDIX. Normalized curves represent the raw data for the linear combination. *A*: receptive field (RF) shift to horizontal apparent motion. Stimuli were 30-ms tone bursts at the unit's best frequency (BF), jumping horizontally across the speaker array at an interpulse interval (IPI) of 66.6 ms at 10 dB above the unit's minimum threshold. Mean response in the contralateral direction of motion (1.046 spikes/stimulus, filled symbols) was not significantly different from that in the ipsilateral direction (1.054 spikes/stimulus, open symbols). However, the normalized data shown at the *bottom* of the figure showed a significant RF shift. Similarity between the *top* and *bottom* graphs indicates that intersweep variability and directional magnitude differences had little effect. *B*: example of directional bias to horizontal FFM [directional index (DI) = 0.287, $P \leq 0.01$]. Stimulus duration was 175 ms, the IPI was 200 ms, and the intensity was minimum threshold (MT) +10 dB. Note the similarity in the 2 curves after normalization (*bottom*) and the size of the error bars. Although some locations in the normalized data exhibit minor differences, there was not a significant shift between the 2 directional receptive fields. *C*: combined shift and directional bias to horizontal FFM. Normalization to sweep total (*bottom*) reduced but did not eliminate directionality. Stimulus configuration was 30-ms duration/66.6 ms IPI, MT +20 dB. Although a directional bias occurred in this set, not all directional effects could be attributed solely to changes in the overall response across all locations. Linear combination on the normalized data was statistically significant, indicating that in addition to the directional bias, there was also a significant RF shift in this set. Note that the response in the ipsilateral hemifield was below the spontaneous firing rate, indicating that this unit had inhibitory ipsilateral input [i.e., was an excitatory/inhibitory binaural response type (EI) unit].

twice the number of spikes than ipsilateral motion (1.85 vs. 0.88 spikes/stimulus). The net result of these changes is a lateral shift between the RFs measured in the two motion directions, manifested by local increases in the response at certain locations and decreases at others.

The location of the receptive field border in DPD cells is considered an important information bearing parameter for encoding sound location based on a population code (Fuzessery and Pollak 1985; Wenstrup et al. 1986). Accordingly, we used the points at which the response was 50% of the peak response (in either direction) to estimate RF border location and used the difference in border location due to motion direction to quantify the magnitude of the RF shift. We refer to the angle between shifted border locations as the "border displacement" in contrast to an "RF shift," which indicates a statistically significant linear combination. In Fig. 2A, the lateral RF border was 48.9°CL for ipsilateral motion and 41.3°CL for contralateral motion (linearly inter-

polating between points), resulting in a lateral border displacement of 7.6°. The medial borders were 6.1°CL for ipsilateral motion and 3.0°IL for contralateral motion, producing a medial border displacement of 9.1°.

Figure 2A, *bottom*, shows the same data after normalization. The high degree of correspondence between the raw data (*top*) and normalized data (*bottom*) is typical of motion effects that only involve RF shifts (i.e., without a directional bias). In this case, analysis using the linear combination technique on the normalized data showed that the difference in the receptive fields was statistically significant.

Apparent motion can produce a directional bias in response magnitude without a RF shift

Similar to previous reports of directional selectivity in the visual and auditory modalities, we found that opposing motion directions also could produce differences in overall

response magnitude. Directional preference, the term commonly used for this effect, generally refers to a response in the preferred motion direction at least twice that in the nonpreferred direction (e.g., Felleman and Kaas 1984; Suzuki et al. 1990). To avoid terminological confusion, we use the term directional bias to refer to the smaller differences we observed.

The example in Fig. 2B shows the largest directional bias observed in this study. The mean response across all locations to contralateral motion (1.301 spikes/stimulus) was significantly different from the mean response to ipsilateral motion (0.927 spikes/stimulus). The normalized data Fig. 2B, bottom, show that the shape of the RF in the two directions of motion was very similar when intersweep variability and magnitude differences were blocked out of the data (cf. Fig. 2A, bottom).

To compare the strength of the directional bias observed here with that in other studies, a directionality index (DI) (Felleman and Kaas 1984; Suzuki et al. 1990; Wagner and Takahashi 1990) was adopted where

$$DI = 1 - (\text{lower response/higher response})$$

The response measure is the mean number of spikes per stimulus across all locations in a given motion direction. As the response in the two motion directions diverges, the value of the DI approaches 1.0, and directional preferences >2:1 would have DIs >0.5. For the example shown in Fig. 2B, the DI was equal to 0.287. Apparent motion sets with a significant directional bias had DIs ranging from 0.048 to 0.287 with a mean DI of 0.128.

We should note here that a directional bias in the absence of a RF shift also could change the location of RF borders due to simple spike count differences across all locations. For example, the directional bias shown in Fig. 2B produced a medial border displacement of 7.2° and a lateral border displacement of 4.4°.

Apparent motion can produce both a RF shift and a directional bias

A third type of directional effect, a combined RF shift/directional bias, also was observed in response to apparent motion stimuli. The example shown in Fig. 2C exhibited a small, but highly significant directional bias ($DI = 0.19$; $P \leq 0.0001$). After normalization to sweep total (Fig. 2C, bottom) the resultant curves still appear different: blocking the directional bias out of the data did not eliminate the directionality as it did for those sets showing a directional bias only (Fig. 2B). Statistical analysis showed that, in addition to the directional bias, there was a significant RF shift after normalization. The combined effects shifted the medial borders of the RFs by 6.2°, and the lateral borders by 1.0°.

Magnitude of border displacement and directional bias

Medial RF border displacements were typically larger than lateral displacements for horizontal motion. Figure 3A shows the medial and lateral border displacement for all significant horizontal motion sets. Although horizontal motion typically revealed “closed” RFs (i.e., the RFs had borders on both the medial and lateral sides), a limited

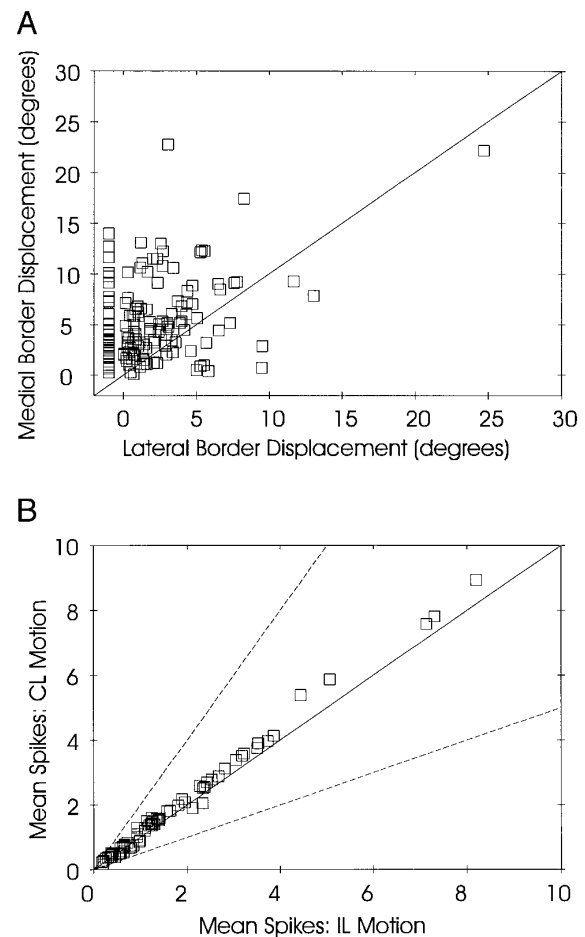


FIG. 3. A: medial vs. lateral border displacement for horizontal FFM. Border displacement is displayed regardless of direction of displacement. Units with open RFs are shown as having a lateral border displacement of -1.0 . Because a directional bias also can produce border displacements (e.g., Fig. 2B), sets with a directional bias in the absence of a RF shift are included in this graph. B: average response magnitude for horizontal FFM sets with a directional bias. Values along the y axis represent the mean response across all locations to contralateral motion and the x axis represents the mean response for ipsilateral motion.

number of units had “open” RFs, which lacked a lateral border (this border was presumably beyond the azimuthal range of the speaker array). For sets with open RFs, the missing (lateral) border displacement is displayed in Fig. 3A as -1.0 . Points above the solid line indicate larger medial than lateral border displacements and represent 80% of all significant horizontal motion sets with closed RFs. The mean and median border displacements for the medial border were 5.35° and 4.32° (range = 22.7°), whereas the mean and median lateral border displacements were 2.98° and 2.15°, respectively (range = 24.7°).

Directional bias, while significant, was small in magnitude. Fig. 3B shows the mean response across all locations for horizontal motion sets with a significant directional bias either alone or in combination with a RF shift. The solid line shows where the spike counts in both directions of motion would be identical, and the dashed lines show where the spike count ratio for the two directions of motion would equal 2:1. Although responses to the two directions of motion were significantly different for all points on the graph,

this figure illustrates how low the DI values were in the FFM paradigm.

Shift direction

In most sets showing significant motion effects, the RF borders were displaced in a direction opposite to the direction of motion, i.e., toward the motion source. For example, in Fig. 2A, the medial RF border was shifted 9.1° toward the source of the motion and the lateral RF border was shifted 7.6° toward the source. The direction of the border displacements for all significant FFM sets with closed RFs are shown in Fig. 4. Positive values indicate displacements toward the source. The clustering of the points in the first quadrant for RF shift alone (Fig. 4A) and for combination shift/bias sets (Fig. 4B) shows that most sets with RF shifts had positive border displacements toward the motion source. For 88% of shift alone and 85% of combination shift/bias sets, entry into the RF from either direction displaced the border opposite the direction of motion. Directional bias-only sets (Fig. 4C) had a more even dispersion among the four quadrants of the graph, indicating that motion direction does not predict displacement direction as accurately as in sets with significant RF shifts. More than one-half of the points were in either the second or fourth quadrant of this graph, indicating mixed positive and negative displacements like those in Fig. 2B, where the lateral border displacement was away from the source. Mixed displacements were much less common in the shift and combination shift/bias sets, ~ 10 and 12% , respectively. In addition, the bias only sets had a high degree of displacement asymmetry, where the border displacement on one side of the receptive field was much larger than on the opposite side. The ratio of the two border displacements was $\sim 10:1$ in sets with a bias alone as compared with $3:1$ for sets with RF shifts and $8:1$ for combined shift/bias effects.

Displacement asymmetry may generate a directional bias

A large border displacement on one side of the RF in combination with a small or nonexistent border displacement on the other might produce a significant directional bias. More symmetric RF displacements such as those seen in the shift-only example in Fig. 2A would offset a larger response on one border for a given motion direction by a smaller response along the other border, equalizing the total response in the two directions of motion. In contrast, highly asymmetric border displacements (e.g., Fig. 2C) would cause a RF shift also to have a greater number of spikes in one direction of motion over the other, generating a directional bias.

Open RFs could be considered an extreme form of displacement asymmetry. For example, the horizontal motion response shown in Fig. 5A shows only a medial border displacement. According to our statistical analyses, there was both a significant shift and directional bias in this set (medial border displacement = 7.3° ; DI = 0.1, $P \leq 0.01$). However, the calculated directional bias might not have been significant had there been an opposing change in activity laterally to offset the change in response documented medially. Open RFs were observed in only 17% of shift-only sets, compared with 23% of combined shift/

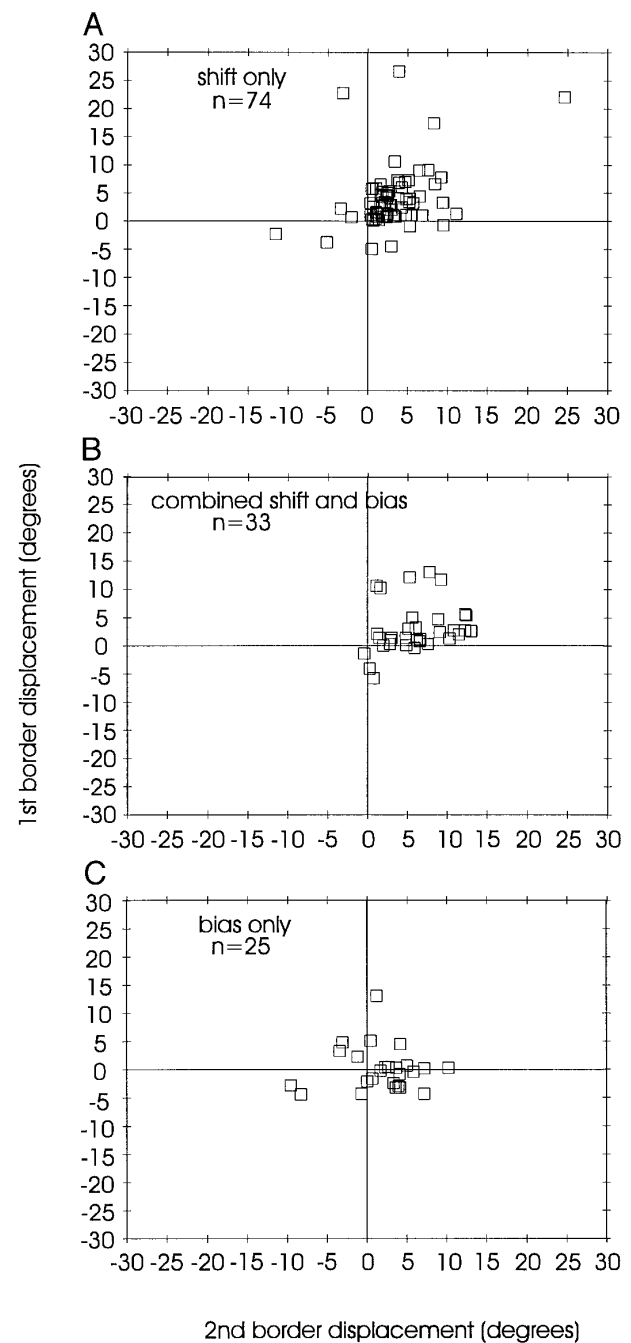


FIG. 4. Border displacements for all sets with significant directional effects and closed RFs. *A*: shift only sets. *B*: combined shift and directional bias sets. *C*: directional bias only sets. Border displacement was calculated from the 50% cutoffs as described in the text. RF border displacement is positive where the borders are displaced toward the source (i.e., opposite the direction of motion). Because motion orientation could vary, the 2 border displacements in a closed RF were arbitrarily assigned to either the 1st border displacement and 2nd border displacement axis. Thus the set shown in Fig. 2B is represented in C at the point (7.2, -4.4). Points in the 1st quadrant have both RF border displacements toward the motion source. Those in the 3rd quadrant have both displacements away from the motion source.

bias sets and 40% of the sets with a directional bias only, supporting the idea that a high degree of border displacement asymmetry gives rise to significant directional bias calculations.

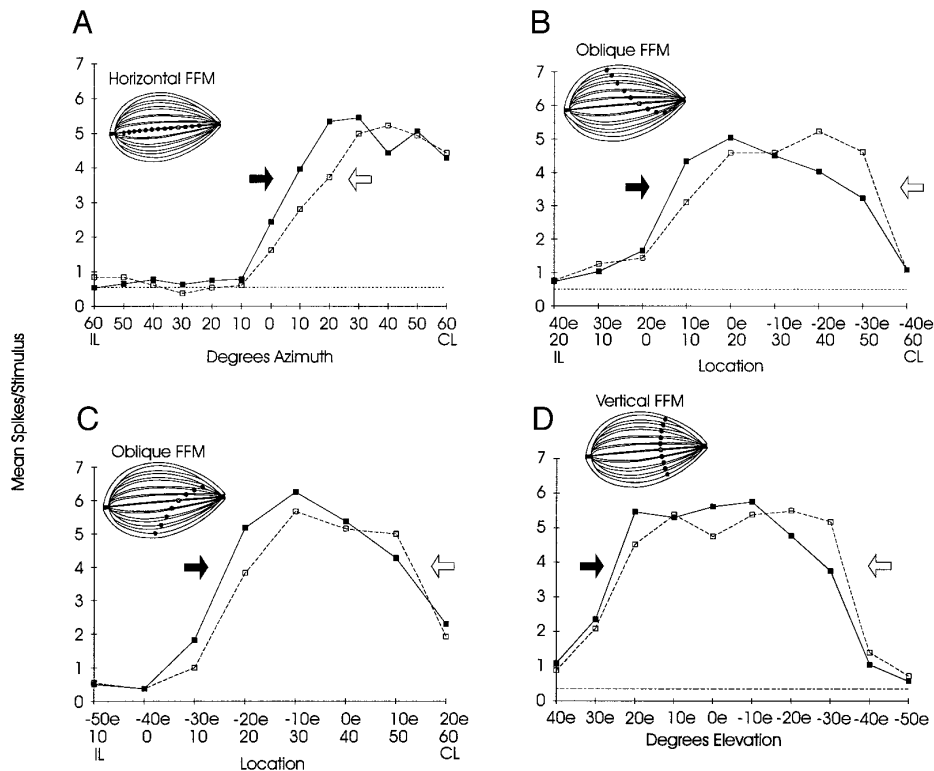


FIG. 5. Directional effects observed across multiple orientations of motion in a single cell. All sets were run at 30-ms duration, 66.6 ms IPI and MT +10 dB. A similar directional effect was observed for vertical and oblique orientations of motion as to horizontal FFM. Entry into the RF elicits a larger response and shifts the RF border toward the motion source. *Inset*: motion orientation. Sets run in the horizontal, left-oblique (upper IL to lower CL), and the vertical orientations (A, B, and D, respectively) showed significant RF shifts. Horizontal and the right oblique (lower IL to upper CL) orientations (A and C) exhibited a directional bias.

Border displacement asymmetry in combination with a consistent displacement direction (Fig. 4, A and B), would explain the slightly larger response to contralateral motion in 82% of horizontal motion sets with a directional bias (Fig. 3B). In neurons with RFs in the contralateral hemifield, RF shifts toward the motion source produce a larger response to contralateral motion on the medial edge of the RF and a larger response to ipsilateral motion on the lateral edge of the RF (e.g., Fig. 2, A and C). Because displacement asymmetry favored the medial over the lateral border (Figs. 2C and 3A), the local directional bias was typically greater on the medial border than the lateral border. Thus contralateral motion should generate a greater overall response in sets with a directional bias, if that directional bias was caused primarily by asymmetric border displacements.

Motion in any orientation produces analogous shifts

The directional effects observed for vertical and oblique motion were qualitatively similar to the horizontal FFM effects already described. Significant directional effects were observed in 70% ($n = 14$) of the 20 units tested with vertical or oblique apparent motion orientations. Figure 5 shows the dynamic receptive fields for a cell tested with the four possible orientations of FFM centered at 30°CL , -10°e . As was the case for horizontal motion (Fig. 5A) sound moving in the vertical (Fig. 5D) and oblique orientations (Fig. 5, B and C) produced a significant directional effect that also displaced the RF borders toward the motion source.

The RF borders in this unit for the four cardinal motion orientations were determined using the 50% points and are shown in the polar plot in Fig. 6A, along with two other examples (Fig. 6, B and C). The solid lines and arrows

show the RF borders for stimuli entering the RF and the dashed lines and open arrows show the borders for stimuli exiting the RF. Because sound moving in any orientation entirely *through* the RF would displace both RF borders toward the motion source, motion *entering* the RF from any point in space should effectively expand the RF borders, and motion *exiting* the RF should contract the RF borders.

Directional effects change with stimulus timing

We varied the temporal characteristics of apparent motion stimuli in some recordings and found an influence on both the probability and magnitude of directional effects. Stimulus duration, IPI, the silent gap between stimuli, and apparent motion velocity covary and no single variable was a simple predictor of the response to apparent motion. In general, however, more consistent and larger effects were obtained for motion with high apparent velocity and with short temporal gaps between individual locations in the stimulus.

Figure 7, A–D, shows the effect of IPI (and apparent velocity) using 30-ms duration stimuli on horizontal motion responses in a single unit. Apparent motion at 300 ms IPI showed no significant difference for the two motion directions. Shorter IPIs of 200, 100, and 66.6 ms, each gave rise to significant RF shifts as well as a small directional bias at 100 ms IPI (Fig. 7, B–D). The average of the RF border displacements increased progressively from 0.8° at 200 ms IPI ($50^\circ/\text{s}$ velocity) to 1.9° at 66.6 ms IPI ($150^\circ/\text{s}$ velocity).

Decreasing the IPI concomitantly decreased the silent gap between stimuli and increased the apparent velocity, although none of these factors were solely responsible for the stronger directionality observed in this unit. This is illustrated by the cell's response to an FFM stimulus with a

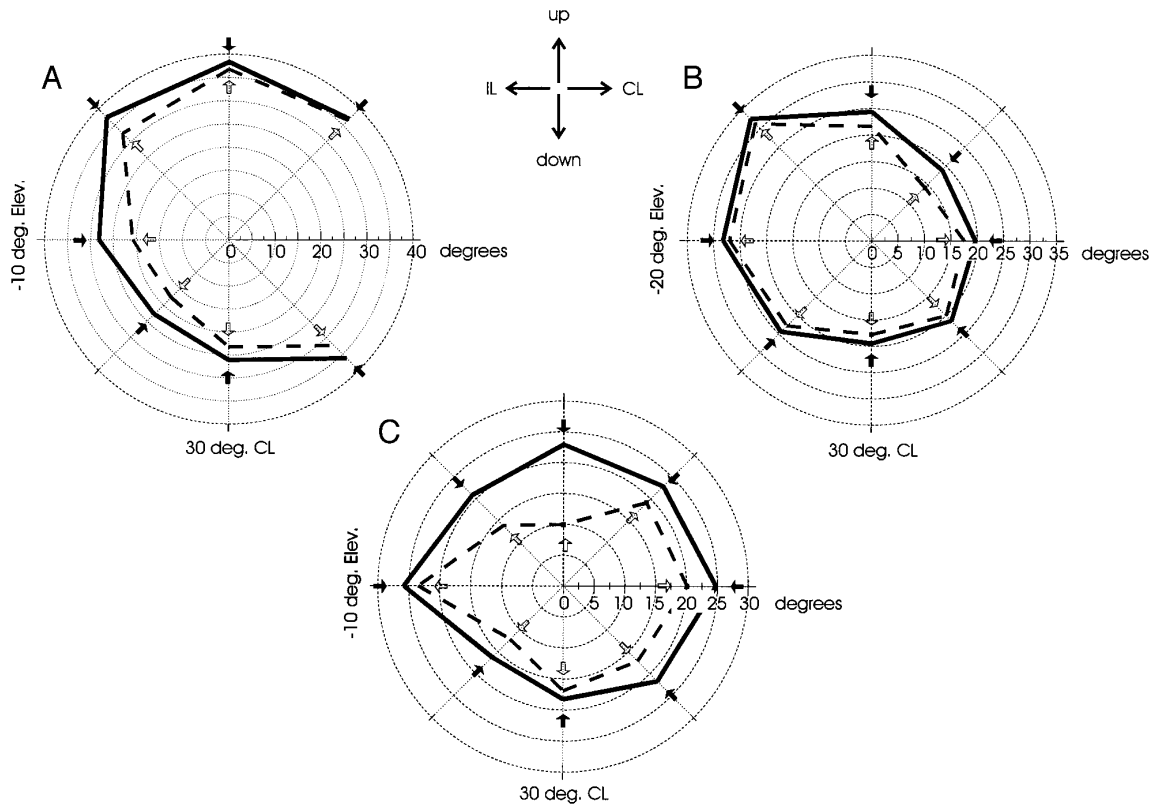


FIG. 6. Polar plots of the RF borders gathered across multiple orientations of motion for 3 single units. Origin of each graph represents the location of the speaker common to all orientations of motion and border locations are shown as angular distance from this point. Solid lines and arrows show the RF borders for motion entering the RF; the dashed lines and open arrow show the RF border locations for motion exiting the RF. RF borders for horizontal motion are shown on the horizontal axis, vertical motion is on the vertical axis, and oblique motion, along the two oblique axes. *A*: RF borders for the data shown in Fig. 5 (*center* of plot = 30°CL, -10°e). Note that this was an open RF and only the medial side of the RF was obtained for horizontal FFM. *B*: FFM was run at 30-ms duration/100 ms IPI, MT +10 dB in this example. Motion in all orientations produced a significant RF shift and horizontal FFM also produced a significant directional bias. *C*: FFM run at 30-ms duration/100 ms IPI, MT +10 dB. Horizontal and lower IL to upper CL orientations of motion exhibited significant shifts.

longer duration (Fig. 7E). Even though the sets in Fig. 7, C and E, had similar the silent gaps between stimuli (70 and 60 ms, respectively), the average border displacement for the long duration/IPI condition (Fig. 7E, 5.33°) was more than three times that of the short-duration/IPI condition (Fig. 7C, 1.65°). Moreover, the sets in Fig. 7, B and E, had the same IPI and apparent velocity, but a much larger average border displacement was observed for the long duration/short gap condition (Fig. 7E, 5.33°; Fig. 7B, 0.8°).

Figure 8A shows that a longer stimulus duration in sets with 200 ms IPI had a higher probability of producing a significant directional effect. One possible explanation for this effect is that longer duration stimuli elicit a greater number of spikes in tonically active units (Fig. 8B) and make directional effects statistically more robust. Figure 8C shows the proportion of sets with a significant directional effect as a function of the average spike count per trial in those sets. The probability of obtaining a significant result increased dramatically with response magnitude, from 38% (average spike count ≤ 500 spikes/trial) to $\sim 78\%$ (average spike count $> 2,000$ spikes/trial). While this strongly suggests that the higher spike counts associated with long duration stimuli contribute to the probability of obtaining a sig-

nificant directional effect, it should be noted that the temporal gap between stimuli decreased at long stimulus durations in Fig. 8A. Thus short temporal gaps also are correlated with the higher likelihood of a directional effect.

Figure 9A shows that motion stimuli with shorter IPIs (and higher apparent velocities) were also more likely to elicit significant directional effects. In this case, however, stimulus duration was held constant at 30 ms and IPI was variable. The probability of obtaining a significant directional effect increased with progressively shorter IPIs. However, the number of spikes/trial was relatively constant at the three IPIs (Fig. 9B), indicating that increased statistical power was not responsible for the higher probability of a significant result. In fact, we commonly observed a decrease in spike counts at shorter IPIs within individual units (e.g., Fig. 7, A–D), which should decrease the probability of obtaining a significant effect in an individual unit. Because silent gap covaried with IPI, the highest probability of obtaining a significant directional effect in Fig. 9A was not only at the shortest IPI but also at the shortest silent gap between stimuli.

Common to both Figs. 8A and 9A is a higher probability of a directional effect with shorter gaps, suggesting that the

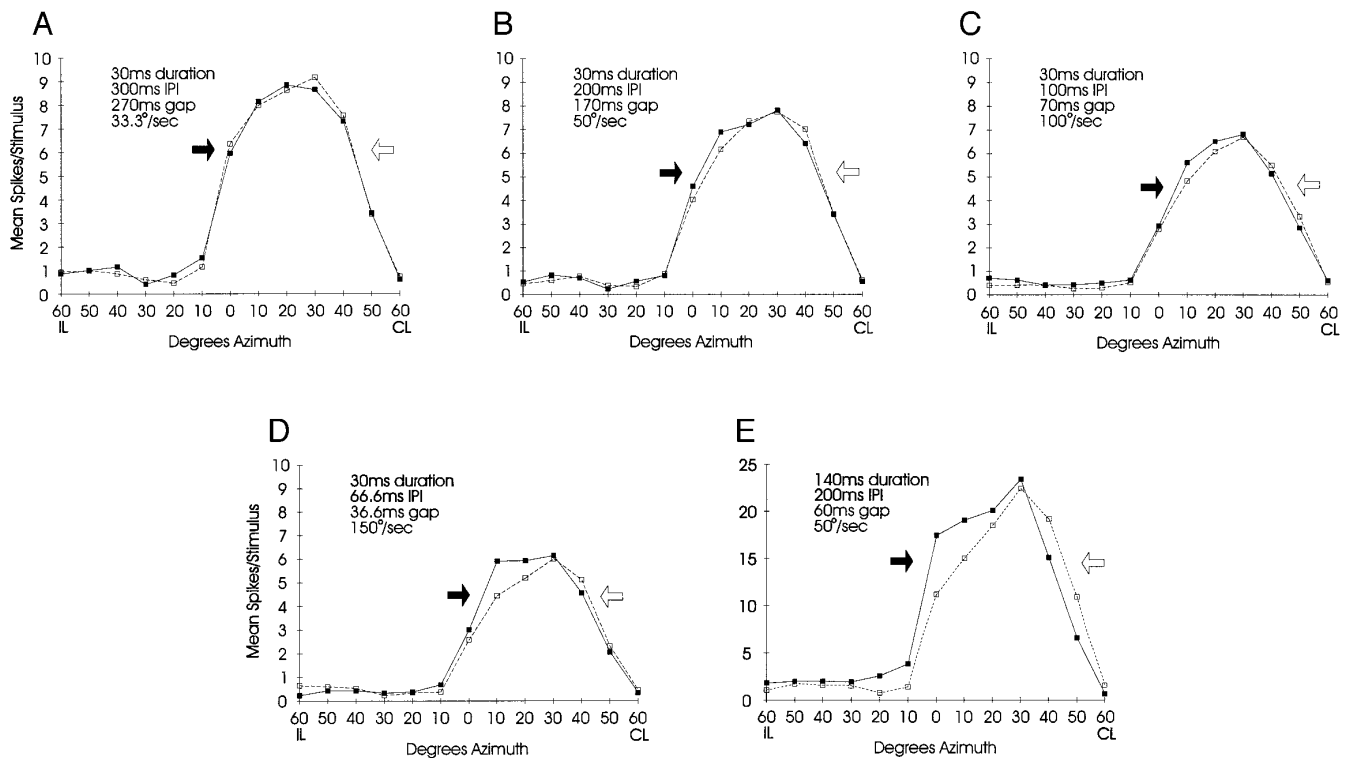


FIG. 7. Effect of IPI (i.e., apparent velocity) and stimulus duration on horizontal FFM directionality in a single unit. *Inset:* stimulus timing. Directional effects increase with smaller temporal gap between stimuli whether produced by decreasing IPI (A–D) or increasing duration (B and E). All sets are horizontal FFM at MT +10 dB. A significant RF shift was observed at IPIs of 200 ms or shorter (B–E). A directional bias (DI = 0.071) also was observed at 100 ms IPI (C) and to the long duration stimulus in (E) (DI = 0.083).

duration of the silent gap between stimuli plays a role in the presence or absence of directional effects. This implies an interaction between the responses to individual tone bursts in the apparent motion sequence and suggests that decreasing the interval between these responses allows for greater interaction.

Although shorter IPIs were more likely to produce directional effects (Fig. 9A), IPI had little influence on the type of directional effect observed (Fig. 9C). Furthermore, the magnitude of the directional bias observed at shorter IPIs did not increase (Fig. 9D). However, the total border displacement for RF shift sets (Fig. 9E) did show a significant difference (one-way analysis of variance; $P \leq 0.01$). A post hoc analysis (Student-Neuman-Keuls test) indicated that the border displacements at 66.6 ms IPI differed from those at both 200 and 100 ms ($P \leq 0.05$).

Directional effects are generated by motion across, but not within, receptive field boundaries

Motion across the entire receptive field had a pronounced effect at the RF edges as demonstrated by the border displacement measurements (see preceding sections). We examined the response to motion in restricted portions of the RF and found that small arcs of motion across RF borders also could elicit directional effects as shown for two cells in Fig. 10. Figure 10, *top*, shows the response of these units to horizontal FFM moving between the edges of the speaker array from 60°CL to 60°IL. A positive border displacement is

evident in both cases, although the effect of motion direction shown in Fig. 10B was not significant. Figure 10, *bottom*, shows the response of these same cells under identical stimulus conditions except that the arc of motion is constrained to the medial border of the RFs. Significant directional effects were observed in both of the partial-arc sets, showing that motion across the border can account for the difference in the response to opposite motion directions and that motion through the entire RF is not necessary to induce directional effects.

Figure 11 shows the effect of constraining the arc of motion within the RF of a single unit. A significant RF shift occurred with horizontal apparent motion through the entire array (Fig. 11A) as well as when the arc of motion included only speakers spanning the edges of the RF (Fig. 11B). However, when only those speakers eliciting a response within the RF were included (Fig. 11C), there was no longer a significant directional effect (although a nonsignificant trend of a smaller magnitude and in the same direction as the previous sets can be seen). Further constraining the arc of motion also failed to produce directional effects (Fig. 11D), showing that motion across RF borders was necessary to produce directional effects.

Response latency also shifts as a function of motion direction

While we have focused on spike counts to illustrate the influence of auditory motion on central auditory neurons, the

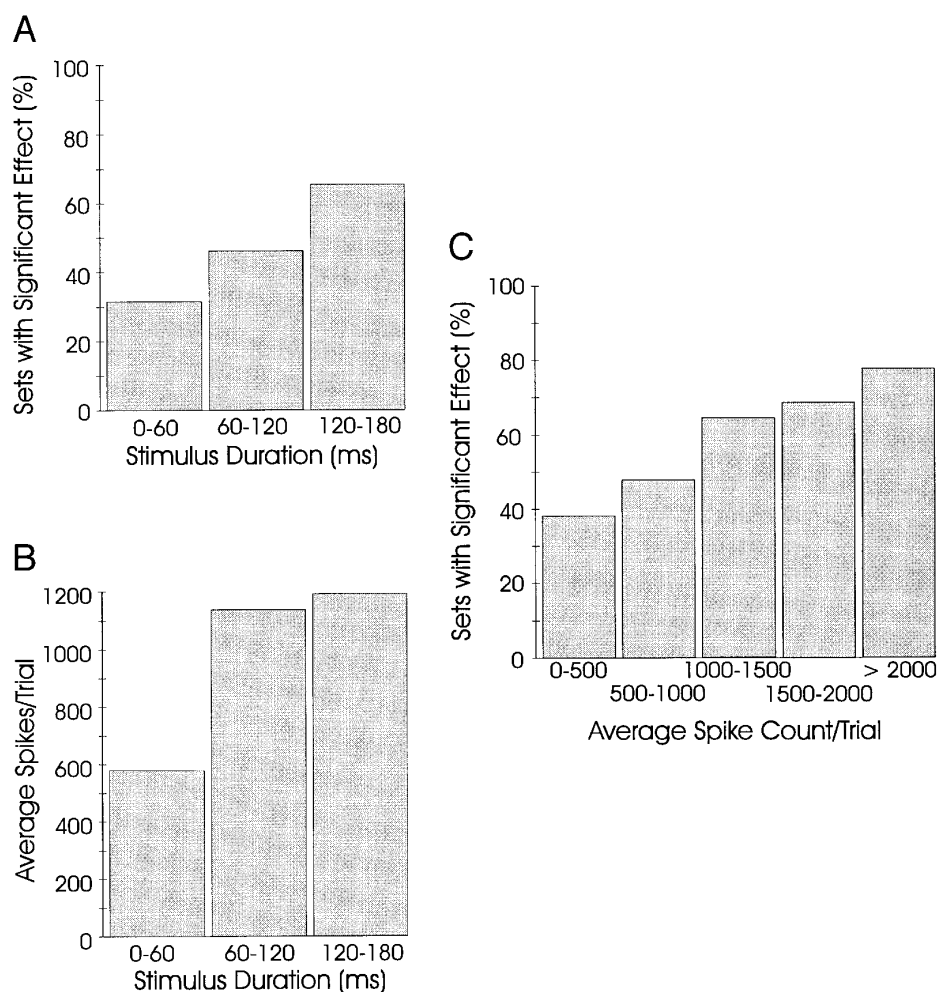


FIG. 8. Effect of stimulus duration on 200 ms IPI sets. *A*: percentage of sets with significant directional effects as a function of stimulus duration for FFM sets with 200 ms IPI. *B*: average number of spikes/trial in the same populations shown in *A*. *C*: effect of response magnitude on directionality. Probability of obtaining a significant directional effect in all FFM sets is shown as a function of mean spikes/trial.

timing of the neural response is also an important descriptor neural response properties (see Brugge 1992 for review). For example, we found that the response latency of single units to stationary stimuli changed with stimulus location (Fig. 12A). This can be explained by the acoustical effects of the head and pinna in combination with the influence of sound intensity on neural response latency. Although we presented stimuli at the same amplitude from all locations, the amplitude measured at the tympanum should vary in a location-dependent manner (e.g., Flynn and Elliot 1965; Musicant et al. 1990). Stimulus amplitudes at the tympanum are greatest when presented from the “acoustical axis” of the pinna, i.e., the location where the stimulus frequency is maximally amplified by the directional properties of the pinna. The amplitude at the tympanum is diminished at off-axis locations.

Because neural latency is inversely related to amplitude (e.g., Møller 1975), the latency to a free-field stimulus should also vary as a function of location. The unit shown in Fig. 12A had a minimum response latency at 30° azimuth, the acoustic axis for 60 kHz in *Pteronotus* (Fuzessery and Pollak 1985). Latency increased by ~1.5 ms at off-axis locations within the RF. Although acoustic path length differences from the different locations to the ear also would influence latency, the maximum acoustic latency difference

produced by the head of *Pteronotus* is only ~0.03 ms for the entire range of the speaker array.

PST histograms for horizontal motion in the same unit (Fig. 12B) show similar characteristics as shown for stationary stimuli: spike counts were highest and latency shortest near the center of the RF, whereas response magnitude was smallest and latency longest at the edges of the RF. However, directionally dependent differences in spike count and latency also can be seen in this figure. Along the medial border of the RF (from 10°IL to 20°CL), motion toward the contralateral hemifield (■) elicited greater spike counts at a shorter latency. Along the lateral border (40–50°CL) the response to ipsilateral motion (□) had a shorter latency. In addition, the response to ipsilateral motion was greater than that to contralateral motion at 50°CL.

These relationships can be seen more clearly in Fig. 12, *C* and *D*, which shows spike count and latency curves for this unit. In general, stimulus locations eliciting greater spike counts (Fig. 12C) also exhibited the shortest neural latency (Fig. 12D). However, in concert with shifting spike count curves, we observed shifting response latencies as a function of motion direction. The effect of apparent motion on latency bears a conspicuous resemblance to the directional effects in the spike count data. Latency is shorter on entry into the receptive field than on exit (regardless of motion direction),

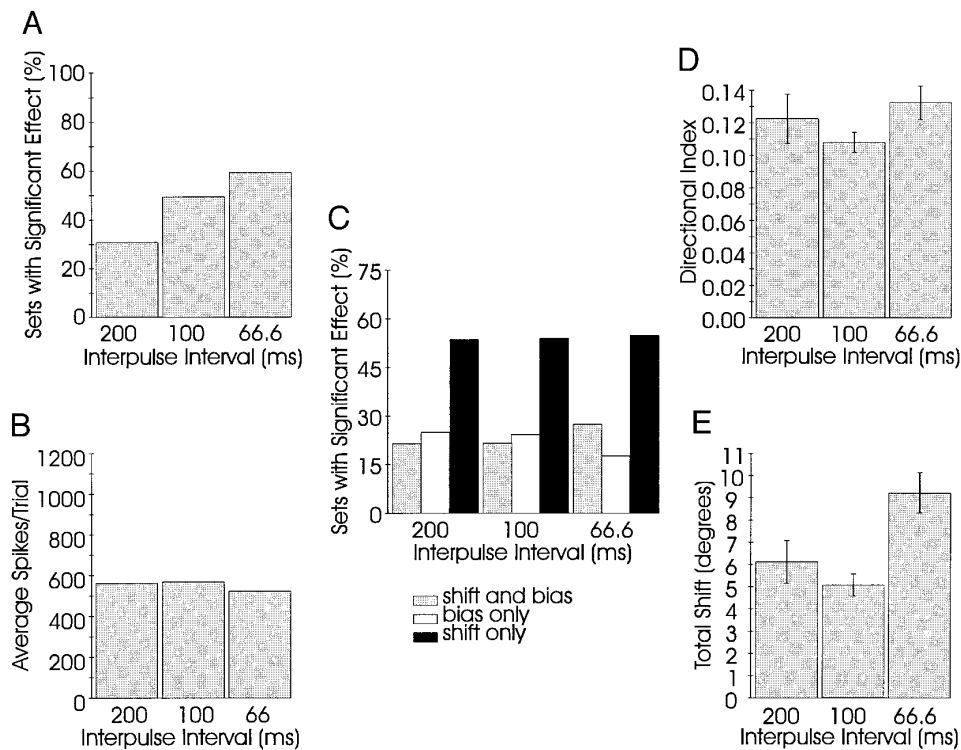


FIG. 9. Effect of IPI on 30-ms duration FFM sets. *A*: percentage of 30-ms duration FFM sets with a significant directional effect shown as a function of interpulse interval. Probability of obtaining a significant difference in opposite motion directions was highest at shorter IPIs. *B*: average response per trial did not increase across the same populations. *C*: effect of IPI on directional effect type for FFM sets with 30-ms duration as a function of interpulse interval. *D*: DI magnitude in 30-ms duration FFM sets with a significant directional bias as a function of IPI. There was not a significant difference between the 3 populations (one-way analysis of variance). *E*: decreasing the IPI to 66.6 ms significantly increased the size of the border displacements observed. Total border displacement measurement used here was the absolute value of the sum of displacements. Thus sets with positive shifts on one RF border and negative shifts on the other have a lower value.

the size of the shift is larger on the medial border than the lateral border, and the latency curves cross at the same location as the spike count curves. Moreover, the directional bias in the spike count data is matched by a similar bias in latency.

DISCUSSION

This study has documented shifting receptive fields and latency profiles in inferior colliculus neurons to auditory motion stimuli. These data illustrate a widespread and consistent influence of motion direction on ICC spatial response properties. Moreover, they demonstrate that the stable receptive fields commonly thought to be a computational substrate for spatial processing are altered by moving sound and suggest that auditory spatial processing is context specific. Our results do not resolve the question of whether motion detectors or directionally selective neurons exist elsewhere within the central auditory system. What our results do show is that the encoding of sound location in the inferior colliculus is significantly modified by motion. We discuss these data further in relation to the information content of dynamic responses and the origin of RF shifts, compare our results to other studies of auditory motion, and discuss the possible influence of RF shifts on the encoding of auditory location. Finally we discuss RF shifts in the context of human auditory motion perception and speculate on the role of dynamic localization "errors" on auditory navigation.

Information in dynamic responses

The physiological response to a moving stimulus is well studied in the visual system and specialization for motion processing is well documented. In primate visual cortex, for example, units responding well to motion in preferred directions and poorly in others are thought to encode motion direction (e.g., Albright et al. 1984; Baker et al. 1981; Felleman and Kaas 1984; Maunsell and Van Essen 1983; Mikami et al. 1986). The present study was motivated, in part, by the question of whether analogous motion processing mechanisms also exist in the auditory domain.

In terms of spike counts, the difference in response between the preferred and nonpreferred direction of motion in our study was only ~13% (average DI = 0.128). If one uses the magnitude of directional preference for visual motion as a benchmark (e.g., Maunsell and Van Essen 1983; Mikami et al. 1986; Suzuki et al. 1990), even the largest directional bias that we observed would be too small to encode motion direction reliably. However, direction is but one of many salient features of a moving stimulus. For example, establishing the direction of a moving sound without also determining its location would be of limited value.

It has been argued that motion has no influence on the spatial response of auditory neurons (e.g., Middlebrooks and Green 1991). Our results suggest the contrary. Whereas the magnitude of the neuronal response to moving sound did not change substantially with motion direction, receptive

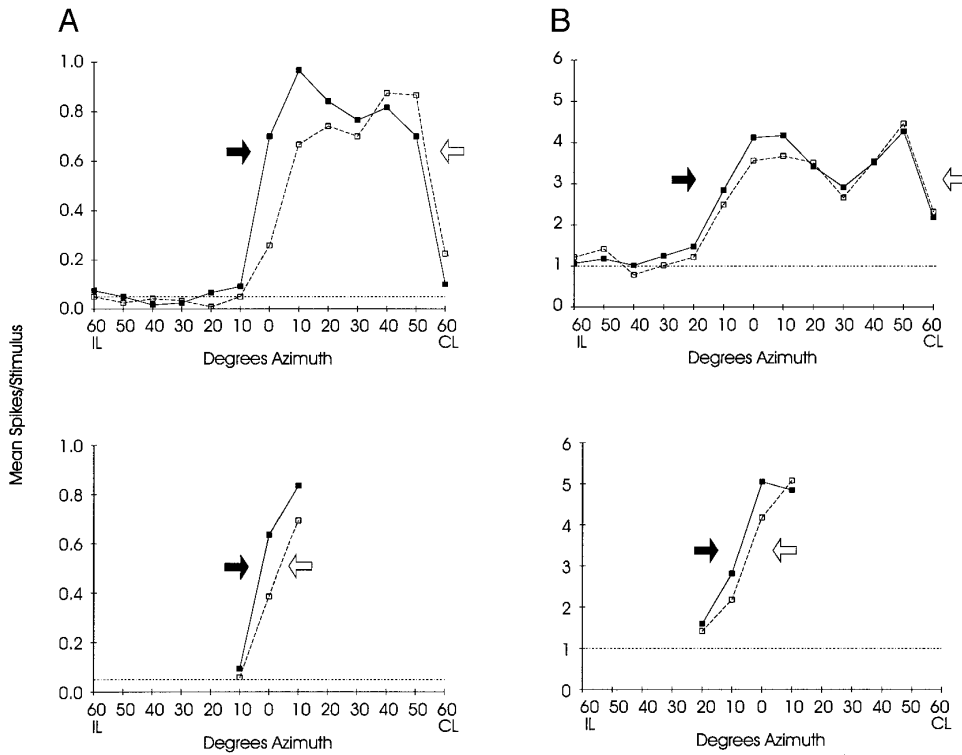


FIG. 10. *Top*: response to horizontal apparent motion across the entire speaker array for two cells. *Bottom*: response of these same cells to motion constrained to the medial border of the RF. *A*: 30-ms duration/66.6 ms IPI at MT +10 dB. Full range motion produced a significant shift and directional bias. Small arc (*bottom*) exhibited a significant directional bias. *B*: 30-ms duration/100 ms IPI at MT +10 dB. Full range motion did not produce significant directional effects. Small arc across the medial RF border (*bottom*) gave rise to both a significant shift and directional bias. Here, both directions of motion in the partial-arc condition were gathered under unidirectional conditions: the response to contralateral motion was obtained by repeatedly presenting contralateral sweeps through the selected speakers separated by 570 ms of silence (produced by inserting 5 “blank” stimulus presentations at the end of each sweep). Response to an equal number of ipsilateral sweeps was gathered in the same fashion. Results were analyzed identically to round-trip motion and found to have both a significant RF shift and directional bias, demonstrating that FFM directional effects were not an artifact of the continuous back-and-forth nature of the typical stimulus presentation.

field boundaries were significantly affected by motion, and in a manner likely to affect the localization of moving sounds, as described below.

Spatial masking

The directional effects described here indicate that prior stimulation at one location alters the response to a subse-

quent stimulus at another location, suggesting some “memory” across locations in the FFM paradigm. We propose that information transfer between locations is produced by the influence of the previous response history on subsequent responses rather than a more direct memory of the previous stimulus. For example, a common characteristic of the greater response to motion toward the center of the RF is a

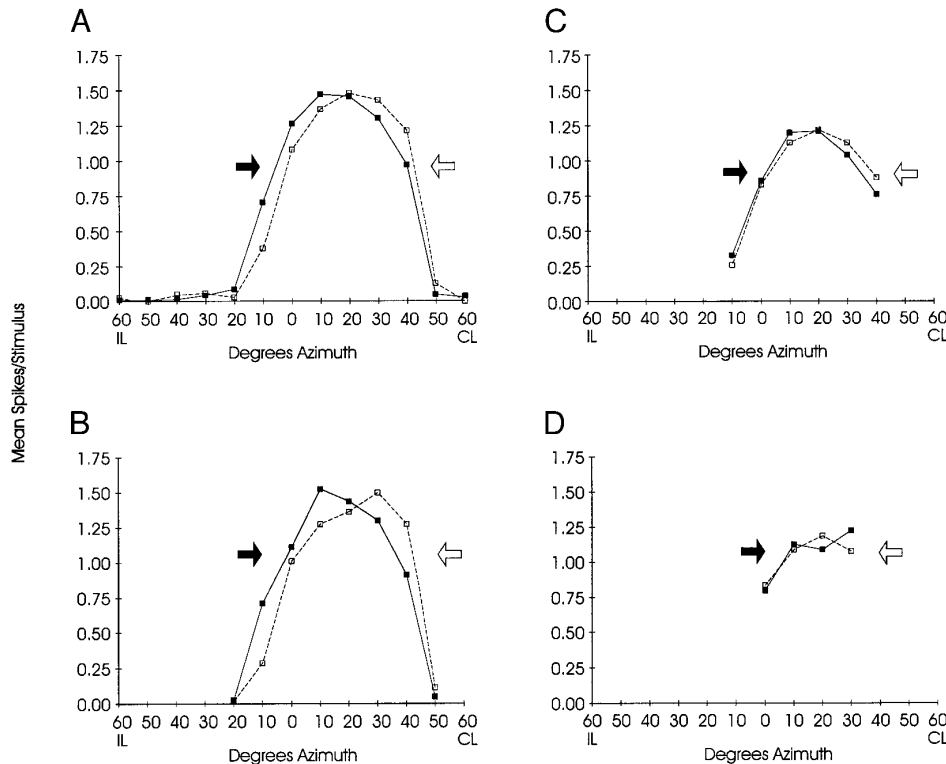


FIG. 11. Constraining FFM within the RF decreases the influence of motion direction. *A–D*: horizontal FFM (30-ms duration/66.6 ms IPI, MT +10 dB) sets with progressively smaller arcs of motion within the RF of a single unit. *A* and *B*: significant RF shift; *C* and *D*: no significant directional effects.

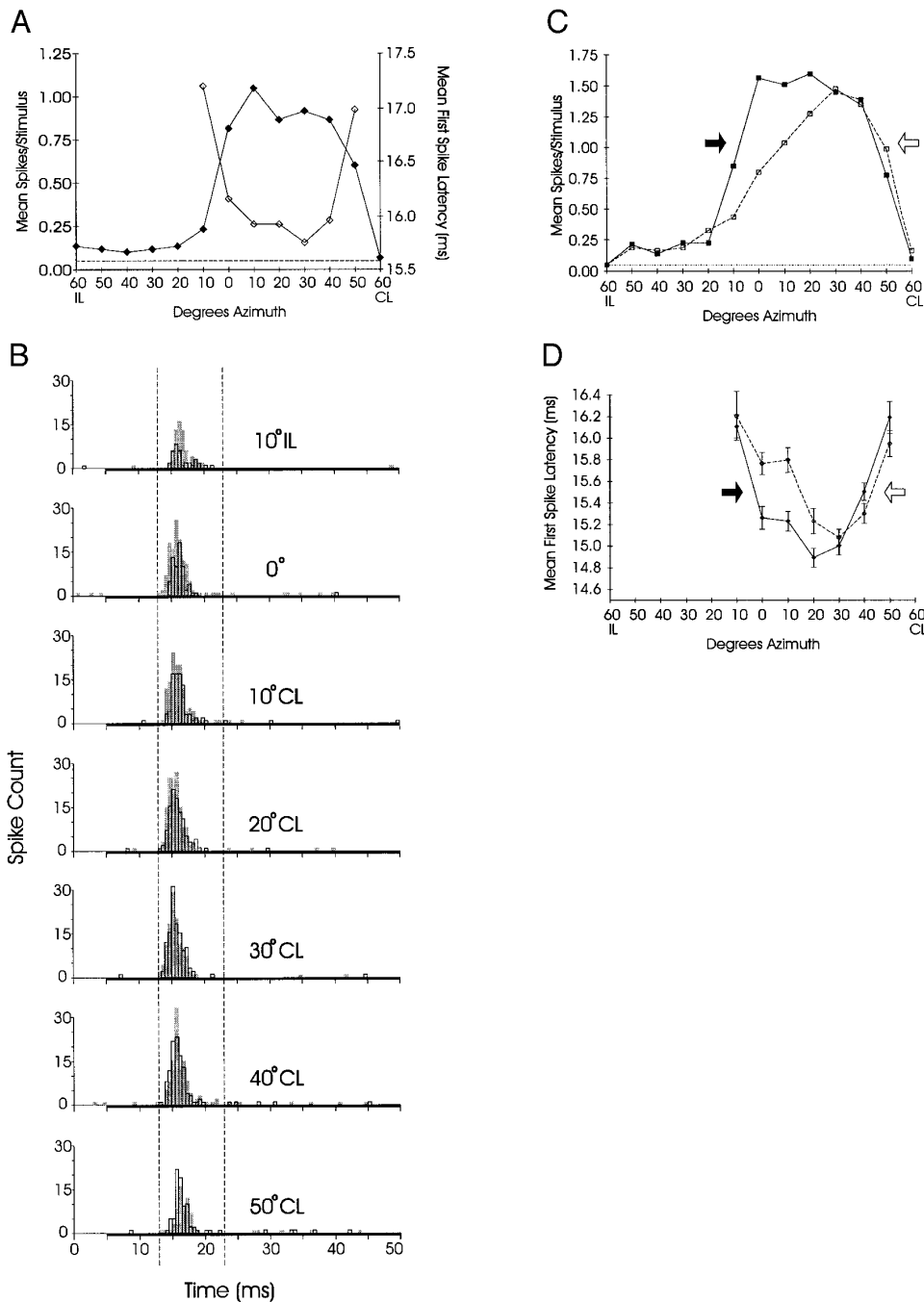


FIG. 12. *A*: static horizontal RF (\blacklozenge) and mean 1st spike latency within the RF (\diamond) for 1 of the 3 SC units. Stimuli were 150-ms duration/200 ms IPI, at MT +10 dB. Medial and lateral borders for the stationary RF were located at 5° IL and 51.4°CL, respectively. To facilitate comparison with the peristimulus time histograms (PSTs; *below*), an additional 6.5 ms was added to the actual neural latency to incorporate the acoustic travel time from the array to the tympanum and a prestimulus acquisition period within the PST (see *B*). *B*: PST histograms for horizontal FFM in the same unit. Stimuli were 150-ms duration tone bursts, at MT +10 dB, presented at an IPI of 200 ms in arcs of motion across the entire array between 60°IL and 60°CL. For clarity, only locations eliciting substantial responses (between 10°IL and 50°CL) have been included in this graph. \blacksquare along the abscissa indicates stimulus onset, and because this unit responded only at the stimulus onset, only the first 30 ms of the response to 150-ms tone bursts are shown. \blacksquare , response to each location to contralateral motion; \square , response to ipsilateral motion; \blacksquare , overlapping bins. The response to contralateral motion across the array can be found by following the dark PSTs from *top* to *bottom* and response to ipsilateral motion by following the light PSTs from *bottom* to *top*. Dashed vertical lines show the temporal windows used for both spike count and latency analysis, from 13 to 23 ms in the PST. Differences in response magnitude and latency can be seen at each location within the RF. *C*: directional spike count function for the data set shown in *B*. For contralateral motion, the medial and lateral RF borders were 10.8° IL and 49.6°CL, respectively. For ipsilateral motion, the medial border was at 0° azimuth and the lateral border was at 52.3°CL. This set exhibited a medial border displacement of 2.7°, and a directional bias with a DI = 0.164. *D*: mean first spike latency as a function of location and motion direction for the same data. Latency at points with low spike counts is uninformative due to high variability and is not shown. Note the close correspondence between the RF shift (*C*) and the latency shift (*D*).

recent history of low response levels to ineffectual or inhibitory stimuli outside the RF; the diminished response to motion away from the RF center has a history of high response levels to excitatory stimuli within the RF. Our results could be explained by "spatial masking," whereby responses to previous stimuli decrease the responsiveness of a cell in proportion to the level of prior activity.

Under this model, the response at a given location in an arc of motion would be determined by at least two sets of factors. The first would be the set of factors normally affecting the spatial tuning of the cell, including the transfer functions of the pinnae, stimulus intensity, and binaural tuning. The ability of the cell to respond fully to this first set of factors would be biased by the second set of factors related

to the spatial masking exerted by previous stimulation on both monaural and binaural spatial tuning. Masking stimuli have been shown physiologically to influence the response to subsequent probe stimuli at the same location (Chimento and Schreiner 1991; Feng et al. 1994; Harris and Dallos 1979; Kiang et al. 1965). Spatial masking would be a motion-specific case of these observations, where masker and probe levels change dynamically within an arc of motion due to the acoustical properties of the head and pinna.

Stationary responses

The responses to stationary stimuli observed in this study were consistent with earlier studies of mustached bat ICC

(Fuzessery and Pollak 1985; Fuzessery et al. 1990; Wenstrup et al. 1988) and generally similar in character to the responses to moving stimuli. Although a complete description is beyond the scope of this report, the temporal response patterns to static and dynamic stimuli were alike and stationary RFs were found in comparable locations to dynamic RFs. For example, both the medial and lateral borders of the stationary RF shown in Fig. 12A were located halfway between their shifted dynamic RF borders (Fig. 12C).

However, a direct point-by-point comparison of static and dynamic responses is confounded by the influence of spatial masking. For example, the effective duty cycle at a given location is very different for static and dynamic stimuli. Horizontal apparent motion across the entire speaker array could spend more than half of each sweep outside of the RF, thereby decreasing the effective duty cycle on the RF borders and reducing spatial masking on the excitatory input to the cell. By contrast, static stimuli at the RF borders consistently drive a cell at the IPI of the stimulus, making it possible for preceding stimuli from the same location to mask the static response. Because the responses to moving and stationary stimuli are determined in part by which locations precede them, a direct comparison of the response magnitude to moving and static stimuli would produce equivocal results.

Comparison with other studies of auditory motion neurophysiology

Previous studies using a variety of techniques have demonstrated the effect of motion in nuclei from the brain stem to the cortex and across a variety of species (Ahissar et al. 1992; Altman 1968; Altman et al. 1970; Gordon 1973; Kleiser and Schuller 1995; Morrell 1972; Rauschecker and Harris 1989; Schlegel 1980; Sovijärvi and Hyvärinen 1974; Spitzer and Semple 1991, 1993; Stumpf et al. 1992; Takahashi and Keller 1992; Toronchuk et al. 1992; Wagner and Takahashi 1990, 1992; Wickelgren 1971; Wilson and O'Neill 1995; Yin and Kuwada 1983). Although all of these studies demonstrate some sensitivity to motion direction or its correlates, given the variety of experimental methods, it is perhaps unsurprising that the nature of the motion response varies between studies.

At one extreme are early reports of specialized motion detectors at the mid- and forebrain levels, similar to motion-specific units described in the visual system (e.g., Hubel and Weisel 1962). These units were thought to signal the presence of motion by a responding well to moving stimuli but remaining insensitive to stationary location (Altman 1968; Gordon 1973; Sovijärvi and Hyvärinen 1974; Wickelgren 1971).

More recent studies, including this one, have revealed units in these nuclei that respond well to moving sound and are sensitive to motion direction but do not corroborate the previously observed specialization for moving stimuli *per se* (e.g., Ahissar et al. 1992; Rauschecker and Harris 1989; Spitzer and Semple 1993; Yin and Kuwada 1983). A less specific response class, directionally selective units, respond well to sound moving in a preferred motion direction but poorly in the opposite direction, regardless of stationary spatial selectivity. Direction encoders have been

reported in many of the studies using free-field motion techniques (e.g., Ahissar et al. 1992; Gordon 1973; Morrell 1972; Rauschecker and Harris 1989; Sovijärvi and Hyvärinen 1974; Wagner and Takahashi 1990, 1992; Wickelgren 1971).

Our results suggest that small differences in response magnitude with motion direction may not necessarily encode motion direction even if highly statistically significant. In visual motion studies, directional selectivity often is defined by an arbitrary but commonly used standard of a response in the preferred direction at least twice that in the null direction (e.g., Felleman and Kaas 1984; Suzuki et al. 1990). Although previous reports of auditory directional selectivity show examples with sizable differences in the response to opposite motion directions, the magnitude of the DIs and the criteria for differentiating directionally selective units from directionally insensitive units are not always reported.

Besides the present study, DIs to free-field motion across a neuronal population have been reported in the barn owl brain stem (Wagner and Takahashi 1992) and the monkey auditory cortex (Ahissar et al. 1992). By our reckoning, the neuronal populations reported in these studies are similar to ours in that most neurons in these studies with significant directional effects had DIs below the 2:1 standard, and many units had DIs within the range observed here. However, in contrast to our results, both of these studies document small but significant populations of units with directional preferences of over 2:1, suggesting that these units encode motion direction. By our calculations, these directionally selective cells constitute ~15% of sampled units in the barn owl brain stem (Wagner and Takahashi 1992) and ~10% of sampled units in the monkey auditory cortex (Ahissar et al. 1992), roughly similar to the incidence of directional selectivity reported in most other studies of free-field motion where DI was not reported.

One possible reason for the lack of directionally selective units in our study is that our stimulus configuration might have been inadequate to expose such selectivity. Other free-field motion studies typically have used broadband stimuli that might activate inhibitory sidebands as the sound moved through the transfer function of the pinnae. Another possibility is that the temporal gaps between stimuli may have been too long in our study to mimic real motion adequately. Wagner and Takahashi (1992) showed that DI increases with shorter temporal gaps between stimuli. Therefore, we might have observed larger DIs if we had been able to present stimuli with shorter temporal gaps. However, Rauschecker and Harris (1989) have found large directional differences in peak response at gap durations comparable with those used in our study.

The direction of free-field motion eliciting the largest response is consistent across studies where direction was reported, suggesting that although the character of the auditory motion response differs between studies, all may be measuring the same underlying mechanism. In the horizontal plane, the predominant preferred direction is toward the contralateral ear in nuclei with mainly contralateral hemifield RFs (Ahissar et al. 1992; Gordon 1973; Wickelgren 1971). Similar to the present study, an increased response along the medial receptive field border for contralateral motion also has been observed in the horseshoe bat (Kleiser and Schuller

1995). This consistent preference across studies for motion toward the predominantly excitatory ear is compatible with the idea of spatial masking.

Studies using dichotic apparent motion also have reported directionally selective responses (Altman 1968, 1980; Altman et al. 1970; Schlegel 1980; Stumpf et al. 1992; Takahashi and Keller 1992; Toronchuk et al. 1992; Yin and Kuwada 1983). Consistent with the motion preference toward the excitatory ear observed in free-field experiments, the directional preferences in many dichotic experiments are for stimuli mimicking motion toward the center of the receptive field (Spitzer and Semple 1993; Stumpf et al. 1992; Toronchuk et al. 1992). Moreover, by overlaying the responses in the two directions of dichotic motion from Takahashi and Keller's (1992) study in the barn owl, we found shifts in their data strikingly similar to the free-field RF shifts observed here. This suggests that in addition to the directional preferences reported by Wagner and Takahashi (1990; 1992) in the barn owl, the response to auditory spatial cues also may shift with motion direction in this species.

Dichotic stimuli typically are considered to mimic only horizontal locations across a limited range of azimuths between the acoustic axes for IID cues, and free-field studies typically have used motion in the horizontal orientation only. These limitations have led to some specific predictions for the effects of a sound moving in the free-field. For example, it has been suggested that monaural "ON" cells with contralateral RFs would prefer sounds moving in the contralateral direction (Stumpf et al. 1992; Toronchuk et al. 1992) because this stimulus would provide increasing intensity to the excitatory ear. This would seem logical, provided that the sound moved between the acoustic axes of the pinnae. However, as these authors point out, motion toward the head also could provide this intensity profile. Moreover, for cells with receptive fields centered at the acoustic axis of the excitatory ear (e.g., Fuzessery and Pollak 1985), sound moving into the receptive field of the cell, *regardless of the direction* from which it entered, would increase the intensity to the excitatory ear. Thus the free-field motion direction producing the greatest response may be defined relative to the RF center rather than by a head-centered coordinate system. The directional selectivity observed in dichotic studies using interaural intensity cues and in free-field studies using horizontal motion then might produce directional effects to motion in any direction through the RF of some cell types (e.g., Fig. 6).

Dynamic auditory localization: RF shifts and localization errors

Because sound location is not encoded at the receptor level, it must be computed using binaural cues. Neurons receiving contralateral excitatory and ipsilateral inhibitory input (EI units) are selective for location through sensitivity to IID (see Goldberg and Brown 1968; Irvine 1992 for review), and IID tuning is mapped systematically across the EI area of the DPD in *Pteronotus* (Wenstrup et al. 1986). Units with high inhibitory thresholds, characteristic of the dorsal EI area, have weak ipsilateral inhibitory input and respond well at IIDs representing all but the most ipsilateral azimuths. Units with lower inhibitory thresholds are found in the ventral EI area. They respond to a smaller range of

IIDs representing more contralateral azimuths. Because free-field responses in EI units are predicted by their IID tuning curves (Fuzessery and Pollak 1985), medial receptive field borders in the DPD EI area should vary from dorsal to ventral in congruence with the systematic variation in inhibitory threshold.

A graphic representation of this relationship is shown in Fig. 13. A sound to the left side of the head provides strong excitatory and weak inhibitory input to the right EI area. Because the sound level at the right, inhibitory ear is below the inhibitory threshold of all but the most ventral units in the right EI area, most neurons on this side would be active. However, the high intensity at the left ear would be above the inhibitory threshold of most units in the left EI area, silencing all but the most dorsal units. Auditory stimuli on the right side of the head should produce the opposite EI area activity pattern, and a sound source directly in front of the bat should produce identical activation patterns in both EI areas. This differential pattern of activation between the two EI areas has been proposed as a neural substrate for determining stimulus azimuth (Wenstrup et al. 1986). It should be emphasized that it is the *border* of a neuron's receptive field that is critical to whether it is included in the active zone in response to sound at a given location, and that our results show that motion has its greatest effect at the borders of the receptive field. Thus the EI area activation pattern, and ultimately the encoding of sound location, would be altered in this model by the shifting RFs produced by auditory motion.

In the absence of any directional effects attributable to motion, the dorsal-ventral extent of EI area activity would be expected to oscillate under conditions of left to right horizontal motion between the acoustic axes of the pinnae in direct accord with the changes in sound location. However, we have shown that motion generates higher-order effects that would alter the pattern of neural activity and perhaps change the perceived location of a sound. Because almost all RF border displacements were toward the source of the moving stimulus, it would seem at first glance that the apparent position of a moving sound also should be offset toward its source. However, integration of the motion-induced RF border displacements into the Wenstrup et al. (1986) model for EI unit localization suggests that motion may actually shift the perceived location of a moving sound toward its destination, opposite to the shift observed in individual neurons (Fig. 14).

This would occur because of the effect motion has on the receptive field boundary. Although the active zones in the EI areas should oscillate to moving sound, there also should be a concomitant lead or lag in the position of the edge of the active zone dependent on motion direction. For example, a sound moving to the right would shift the RF borders of cells in the EI areas on both sides toward the left. Consequently, the active zone in the left EI area would shift ventrally (more units would be active) and the active zone in the right EI area would shift dorsally (fewer units would be active), a pattern typical of locations further to the right of the actual stimulus location. Sound moving toward the left would shift the RFs in the opposite direction, again shifting the EI area activation pattern to one more typical of locations along the motion trajectory.

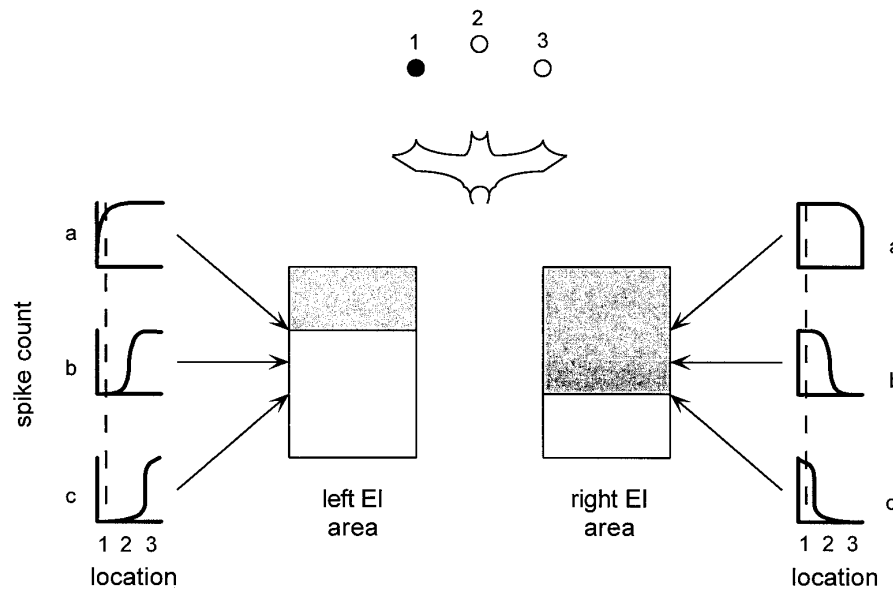


FIG. 13. Wenstrup et al. (1986) model of EI area activation resulting from different azimuthal locations. Spatial tuning based on interaural intensity difference (IID) functions at different dorsal-ventral locations through the right and left EI areas is shown by representative cells *a–c* for 3 azimuthal locations labeled 1–3. Dorsal EI units (*a*) have the broadest spatial tuning and are inhibited by only the most ipsilateral azimuths, whereas ventral EI units (*c*) are only active to the most contralateral stimuli. A stimulus at location 1 would be within the excitatory RF of most units in the contralateral EI area on the right side of the brain and only the most dorsal units in the left, ipsilateral EI area (dashed vertical lines), producing the activation pattern shown by the dark shading. Location 2 would elicit activity in more ventral units in the left EI area (*cell b* now would be active) and no longer activate the most ventral units in the right EI area (*cell c* would no longer be active). Thus a midline stimulus should produce activity in the EI areas on both sides to the level of *cell b*, midway through the dorsal-ventral extent. A stimulus at location 3 should produce an activation pattern opposite that produced by stimuli at location 1, in which units dorsal to *cell c* in the left EI area would be active while only units dorsal to *cell a* in the right EI area would be active.

Influence of latency shifts

The motion-induced latency shifts that we observed also would produce different EI area activity levels for a given location. Motion to the right would be entering the RF of left EI area units, eliciting responses at shorter latencies. The same stimulus would be exiting the RF of right EI area units, eliciting responses at longer latencies. The direction-dependent timing of these responses would serve to temporally shift the EI area activity pattern to one more typical of a location occurring at an earlier time in the motion sequence (i.e., toward the motion source). However, this effect should be negligible in comparison with the effect of the shifting spike count functions described above. In the example shown in Fig. 12D, the largest difference in neural latency between the two directions of motion was ~ 0.5 ms. This should produce a location shift of 0.025° at $50^\circ/\text{s}$, an extremely small effect compared with the medial border receptive field displacement of 10.8° in this same data set.

However, because sound sources and listeners are commonly in motion, direction dependent latency shifts might influence any number of other auditory processes that rely on coincident neural response timing (e.g., Phillips et al. 1985). Regarding auditory localization, motion-induced changes in the timing of auditory responses might alter localization based on time cues in the envelope of high-frequency sounds (Batra et al. 1989; Joris and Yin 1995; Yin et al. 1984). In echolocating bats, target distance is computed from the elapsed time between the outgoing sonar pulse and the returning echo, and “range-tuned” neurons are relatively

common in the mustached bat mid- and forebrain auditory system (Mittman and Wenstrup 1995; Olsen and Suga 1991; O’Neill and Suga 1982; Suga and O’Neill 1979; Yan and Suga 1996). Such tuning is thought to be created by pathways differing in neural latency (Suga 1990), and small changes in the timing between simulated pulse/echo stimuli have a profound effect on the response of range-tuned units. Motion-induced shifts in echo latency might similarly alter the response of range-tuned units and thereby produce errors in target ranging.

Comparison with psychophysical studies of auditory motion

The neurophysiological model suggesting that the encoded location of a moving sound is displaced in the direction of motion is consistent with human psychophysical results showing that the perceived location of a moving sound is indeed displaced in the direction of motion (Perrott and Musicant 1977, 1981). Like our physiologically measured RF shifts, psychophysical localization shifts increased as a function of stimulus velocity, reaching a maximum of $\sim 17^\circ$ at $600^\circ/\text{s}$ (Perrott and Musicant 1977, 1981). For 30-ms stimuli, we observed average medial border displacements of $+4.4$ and $+4.8^\circ$ at velocities of 50 and $150^\circ/\text{s}$, respectively. Correcting for travel time from the stimulus source to the listener in their estimates of the localization shift, these values are remarkably similar to the 4.9° (at $45^\circ/\text{s}$) and 6.33° (at $120^\circ/\text{s}$) shifts observed by Perrott and Musicant (1981). The close correspondence between the direction, magnitude,

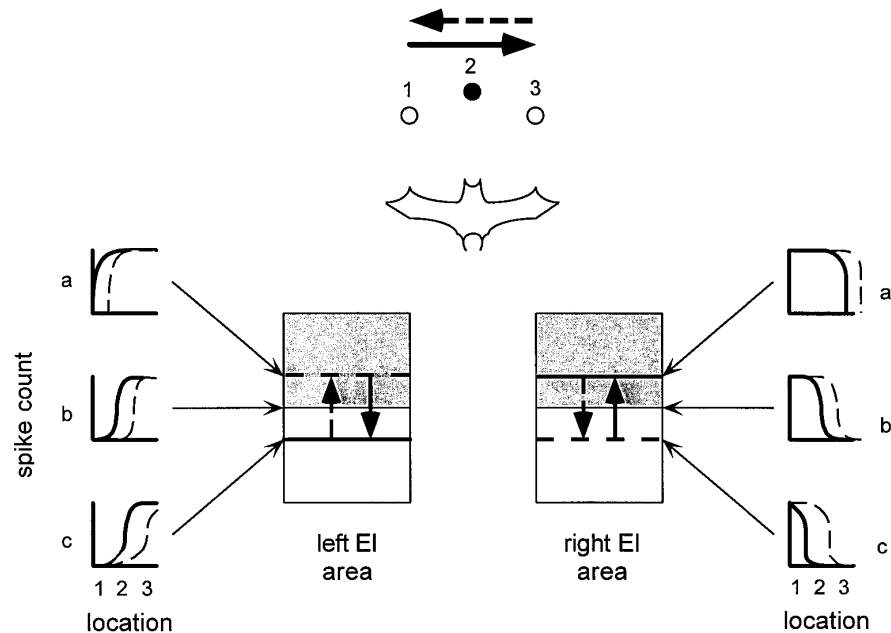


FIG. 14. Expected EI area activation to moving stimuli. Shaded area in the left and right EI areas shows the expected activity for a stationary stimulus at *location 2*, along the midline. For motion to the right (arrow at the *top* of the graph), the RF borders in both the left and right EI areas would shift to locations to the left as observed in the present study (solid RF borders in cells at levels *a-c* in both the left and right EI areas). Motion to the left (dashed arrow) shifts RF borders to locations to the right (dashed RF borders at levels *a-c*). Consequently, a sound at midline (*location 2*) moving toward the right would be within the RF of more units in the left EI area (more ventral cells would be active than for stationary stimuli, shown by solid horizontal line in the left EI area at level *c*) and would be within the RF of fewer units in the right EI area (fewer ventral cells would be active, as shown by the solid horizontal line in the right EI area at level *a*), shifting the pattern of activation toward that typical of stationary stimuli further to the right (i.e., at *location 3*). A sound at midline (*location 2*) moving toward the left would shift the active zones in opposite directions, to the levels shown by the dashed horizontal lines in the EI areas. This pattern is more typical of a stationary stimulus further to the left (along the path of motion) than the actual stimulus location.

and velocity effects in the RF shifts we observed and human dynamic localization errors demonstrated psychophysically, suggests that RF shifts could produce perceptible localization shifts for moving stimuli.

Predictive localization

Between successive echoes, the relative angular velocity of a stationary target 0.25 m lateral to the flight path of a passing bat computes to $\sim 10^\circ/\text{s}$ at a distance of 3.0 m to $>700^\circ/\text{s}$ just before passing the object, using a flight speed (4.5 m/s) and sonar pulse emission behavior typical of *Pteronotus* (Novick and Vaisnys 1964). Thus the apparent motion velocities used in the present report should be well within the range of those normally experienced by *Pteronotus* in flight. Although no data exist on the behavioral acuity for stationary horizontal localization in *Pteronotus*, estimates of 1.5° from another bat species (Simmons et al. 1983) suggest that the RF shifts reported here of almost 5° at $150^\circ/\text{s}$ would represent a substantial potential “error” in localization. The increase in RF shifts with velocity seen in our data, in addition to the very large localization shifts observed in humans at high motion velocities, suggest that RF shifts could be of considerable influence on the localization of a moving sound by a flying bat.

However, a shift in perceived target location caused by auditory motion actually might be exploited by auditory

predators like *Pteronotus*. Some echolocating bats use predictive prey tracking strategies (Campbell and Suthers 1988), and such prediction might be built-in to localization shifts produced by motion. Because the perceived location of a moving target would be shifted toward its destination by the RF shifts, a moving target would have a perceived location ahead of its actual position along the motion trajectory. This might allow the bat to direct its flight in a course that would intercept the target rather than simply follow in its wake.

In conclusion, we have found that the majority of neurons within a hypertrophied isofrequency contour of the mustached bat IC are responsive to apparent motion. The response differs according to the motion direction and takes the form of a shift in the border of the receptive field toward the source of the motion (RF shift), a higher overall firing rate for contralateral motion (response bias), or a combination of the two effects. A similar effect of motion was found on the response latency, in that motion in one direction elicited responses sooner than motion in the opposite direction. Stimuli with higher velocities of apparent motion and shorter gaps between stimuli elicited stronger directional effects. Although we found no cells that responded exclusively to moving sound sources or a given motion direction, the pervasive effect of motion on receptive field borders suggests that motion alters the underlying code for location resident in the population of IC neurons. The net effect of motion

may be to shift the perceived location of a moving sound farther along the motion trajectory than it actually is, consistent with a predictive strategy for interception.

APPENDIX

Variables

p	number of points (i.e. speaker locations) in a motion stimulus. There were $2p$ points in each round-trip sweep (each speaker was activated in both the forward and reverse direction)
n	number of round-trip sweeps in a trial (subdivided into forward and reverse portions)
t	number of trials in a pooled set
$N = n*t$	number of sweeps in a set
i	index for locations
j	index for sweeps
F_{ij}	the observation at the i th point during the forward portion of the j th sweep
R_{ij}	the observation at the i th point during the reverse portion of the j th sweep
TF_j	the total number of spikes during the forward portion of the j th sweep
TR_j	the total number of spikes during the reverse portion of the j th sweep
T_j	the total number of spikes during the j th sweep

Pooling motion trials

We tested for a difference in the response between trials using nonparametric Kruskal-Wallis tests (Sokal and Rohlf 1981) on the spike count distribution at each point i for the forward sweeps, the reverse sweeps, and the difference between the forward and reverse sweeps. The tests on the forward and reverse distributions tested the null hypothesis that the proportion of the total response in a sweep of a given motion direction at point i was the same between trials. The tests on the difference data tested the null hypothesis that the difference in the response in the two directions of motion at point i was the same between trials. We tested to an overall $\alpha \leq 0.05$ using Bonferroni correction. Before testing the $p*t$ forward and $p*t$ reverse distributions, the responses at each point were normalized. The normalization minimized the effect of changes in the responsiveness of the cell between sweeps and assumed that the responsiveness did not change within a sweep. If there was no difference in the response between sweeps, the normalization procedure did not affect the results of the Kruskal-Wallis tests; only the effect of a systematic trend or random variability in the cell's responsiveness between sweeps would be reduced or eliminated by normalization in the pooling procedure. The normalization converted the observed response at each of the locations in a given sweep and motion direction to its proportion of the total response in that direction sweep. Expressed mathematically

$$g(F_{ij}) = \frac{F_{ij}}{TF_j} \quad \text{and} \quad g(R_{ij}) = \frac{R_{ij}}{TR_j}$$

The distributions of the difference at each point between the forward and reverse responses ($F_{ij} - R_{ij}$) for the t trials also were tested for pooling. Normalization was not carried out on the difference data to compensate for the prior normalization of each direction individually. Without the difference test, it would be possible for normalized trials with identical responses in one direction, and response curves with similar shapes but different magnitudes in the other direction to be pooled. Difference measures did not require normalization due to the assumption that the responsiveness of a cell did not change within a sweep.

Aberrant trials were removed from the set and the remaining

trials were tested for pooling validity. If pooled trials for a given set of stimulus parameters fell into subsets of equal sizes (s) and further analyses agreed in all subsets, that result was reported as a single set of size s . In 0.9% of all sets tested for pooling, analysis of equal sized subsets showed conflicting results; these data were not included in further analysis. All subsequent analyses were performed on the largest statistically valid set.

Magnitude effects

The Wilcoxon signed-rank test was used to test whether the response magnitude to the forward sweeps of motion in a set differed from that to the reverse sweeps without regard to the particular locations at which this effect may have occurred. To reduce the effect of any variability in the response between sweeps, the forward and reverse totals for each sweep were paired. Therefore, the overall response on the j th reverse sweep was subtracted from the overall response on the j th forward sweep ($TF_j - TR_j$) resulting in N difference measures in a set. The Wilcoxon signed-rank test was used to test the null hypothesis that the median of the differences was significantly different from zero at a significance level of $P \leq 0.05$.

Linear combination

Initial experiments showed another possible effect of apparent motion to be a shift in the location of the receptive field of a cell for the forward and reverse directions of motion with or without a coincident directional bias. A custom procedure, devised in collaboration with James Colton of the Rochester Institute of Technology, was used to ascertain whether such a shift was statistically significant using a linear combination technique. The linear combination was designed to detect a lateral shift in the receptive field curves by testing for a consistent pattern in the difference between them.

The example in Fig. 2A shows the response of a cell to the two directions of FFM plotted as a function of free-field location. For this discussion, the forward response is shown by the solid line and the reverse response is shown by the dashed line. In developing a curve shift test, it was important to examine *patterns* in the directional responses rather than to test for differences in individual points on the curves. This was because the response at individual points on the curves might differ due to random variability; i.e. the curves might cross at numerous points rather than exhibit a systematic lateral shift. The linear combination technique tested for a shift between the directional responses using the difference in the directional response ($F_{ij} - R_{ij}$) as a measure. It tested for a pattern in the area between the curves, allowing for, but not requiring, the curves to cross at a single point.

Similar to the Wilcoxon and pooling procedures, the test for a curve shift paired the responses by sweep to reduce the effect of intersweep response variability. In addition, the point responses were normalized to eliminate the effect of any directional bias, making the linear combination a test for a consistent pattern in the area between the forward and reverse curves due solely to lateral RF shifts. Because the difference in response magnitude was previously checked with the Wilcoxon test, response magnitude information was blocked out of the linear combination but not lost. The observed directional biases were multiplicative (e.g., $F_{ij} = c*R_{ij}$), rather than additive (e.g., $F_{ij} = c + R_{ij}$). Therefore, the point responses were normalized to their proportion of the sweep response rather than by subtracting a constant from the point response values. The normalization had the effect of making the linear combination a test on the curve shapes rather than a test of the overall difference in the curves.

The measure of the difference between the two directions of motion at point i on sweep j equaled the response at point i in the

forward portion of sweep j normalized to its proportion of the response at all locations in the forward portion of sweep j minus the response at point i in the reverse sweep j normalized to its proportion of the total response in the reverse direction on sweep j . Expressed mathematically

$$g(F_{ij}, R_{ij}) = \left[\frac{F_{ij}}{TF_j} - \frac{R_{ij}}{TR_j} \right]$$

A weighting factor was applied to the difference measures to minimize the influence of locations that elicited a low or no response but would disproportionately contribute to the variability of the measure. This was especially important for cells with a comparatively low driven rate relative to the background firing rate. The weighting factor needed to be indicative of the total response at the i th point while accounting for intersweep variability. Therefore, we used the sum of the forward response plus the reverse response at point i on sweep j divided by the total response at all points during sweep j . The weighted measure of the difference in the two directions would now be expressed as

$$g(F_{ij}, R_{ij}) = \left[\frac{F_{ij}}{TF_j} - \frac{R_{ij}}{TR_j} \right] \left[\frac{F_{ij} + R_{ij}}{T_j} \right]$$

To calculate a measure of the directional curve shift in a motion set, the weighted difference measures were first summed for each point and then summed across all points to yield a value equal to the sum of the directional differences across all sweeps and points

$$LC = \sum_{i=1}^p \sum_{j=1}^N \left[\frac{F_{ij}}{TF_j} - \frac{R_{ij}}{TR_j} \right] \left[\frac{F_{ij} + R_{ij}}{T_j} \right]$$

This is a good measure of the directional difference only for curves that do not cross. For example, in the curve shown in Fig. 2A, $(F_{ij} - R_{ij})$ would have a positive sign on the points on the contralateral/ipsilateral side of the RF and a negative sign on the ipsilateral/contralateral side. This would result in a linear combination that underestimated the actual area between the forward and reverse curves. To obtain a linear combination that was resistant to this effect, p linear combinations were calculated for each motion set with a systematic reversal of the sign of adjacent locations. The first combination computed the sum of all point differences across all locations and sweeps in a set as described earlier. The second combination computed the sum of the negative of the first point differences plus the $(p - 1)$ remaining point differences. The third combination negated the first two point differences and the p th combination negated the first $(p - 1)$ point differences. The largest non-zero sum would result from the linear combination with opposite signs on either side of the point where the curves crossed. In the example in Fig. 2A, the largest linear combination resulted from the ninth iteration of this sequence, where opposite signs were applied to the point differences on either side of the crossover. Thus if S_i equals the sign for the i th point, then the linear combination is calculated as

$$LC = \sum_{i=1}^p \sum_{j=1}^N S_i \left[\frac{F_{ij}}{TF_j} - \frac{R_{ij}}{TR_j} \right] \left[\frac{F_{ij} + R_{ij}}{T_j} \right]$$

The variance of the linear combination was calculated as the sum of the sample variances at each point. This would be expressed as

$$S_{LC}^2 = \sum_{i=1}^p \frac{\sum_{j=1}^N \left(\left[\frac{F_{ij}}{TF_j} - \frac{R_{ij}}{TR_j} \right] - \left[\frac{F_{ij}}{TF_j} - \frac{R_{ij}}{TR_j} \right] \right)^2}{n - 1}$$

The calculated variance was used to construct 95% confidence

intervals for the values of each of the linear combinations using Bonferroni correction for the p combinations. If a given confidence interval did not include zero, the null hypothesis that the true mean of the directional differences at all points and all sweeps was equal to zero was rejected (i.e., the area between the curves was significantly different from 0).

We thank R. A. Eatock, J.H.R. Maunsell, R. C. Emerson, R. D. Frisina, Jr., J. P. Walton, and C. F. Moss for guidance and support on this project and for critical reading of previous drafts of this work. We are indebted to J. Colton for statistical development, H. D. Lesser for the real-time data acquisition software ("HAL"), M. Gira for design and development of the speaker array computer interface, and D. Kurtz for building the speaker array frame. We thank J. L. Ringo and C. E. Carr for scientific advice, K. Karcich for programming advice, and M. Perotto for administrative assistance. We are also grateful for the insightful suggestions of two anonymous reviewers for improving the manuscript.

W. W. Wilson was supported by a predoctoral National Research Service Award (1-F31-MH-10107) from the National Institute of Mental Health.

Present address of W. E. O'Neill: Dept. of Neurobiology and Anatomy, University of Rochester School of Medicine and Dentistry, Rochester, NY 14642.

Address for reprint requests: W. W. Wilson, Dept. of Psychology, University of Maryland, College Park, MD 20742.

Received 30 September 1996; accepted in final form 30 December 1997.

REFERENCES

- AHISSAR, M., AHISSAR, E., BERGMAN, H., AND VAADIA, E. Encoding of sound-source location and movement: activity of single neurons and interactions between adjacent neurons in the monkey auditory cortex. *J. Neurophysiol.* 67: 203–215, 1992.
- ALBRIGHT, T. D., DESIMONE, R., AND GROSS, C. G. Columnar organization of directionally selective cells in visual area MT of the macaque. *J. Neurophysiol.* 51: 16–31, 1984.
- ALTMAN, J. A. Are there neurons detecting direction of sound source motion? *Exp. Neurol.* 22: 13–25, 1968.
- ALTMAN, J. A. Psychophysical and neurophysiological data on the sound source perception. In: *Neuronal Mechanisms of Hearing*, edited by J. Syka and L. Aitkin. New York: Plenum, 1980, p. 289–299.
- ALTMAN, J. A., SYKA, J., AND SHMIGIDINA G. N. Neuronal activity in the medial geniculate body of the cat during monaural and binaural stimulation. *Exp. Brain Res.* 10: 81–93, 1970.
- BAKER, J. F., PETERSEN, S. E., NEWSOME, W. T., AND ALLMAN, J. M. Visual response properties of neurons in four extrastriate visual areas of the owl monkey (*Aotus trivirgatus*): a quantitative comparison of medial, dorsomedial, dorsolateral, and middle temporal areas. *J. Neurophysiol.* 45: 397–416, 1981.
- BATRA, R., KUWADA, S., AND STANFORD, T. Temporal coding of envelopes and their interaural delays in the inferior colliculus of the unanesthetized rabbit. *J. Neurophysiol.* 61: 257–268, 1989.
- BRUGGE, J. F. An overview of central auditory processing. In: *The Mammalian Auditory Pathway: Neurophysiology*, edited by A. N. Popper and R. R. Fay. New York: Springer-Verlag, 1992, p. 1–33.
- BURTT, H. E. Auditory illusions of movement—a preliminary study. *J. Exp. Psychol.* 2: 63–75, 1917.
- CAMPBELL, K. A. AND SUTHERS, R. A. Predictive tracking of horizontally moving targets by the fishing bat, *Noctilio leporinus*. In: *Animal Sonar: Processes and Performance*, edited by P. E. Nachtigall and P.W.B. Moore. New York: Plenum, 1988, p. 501–506.
- CHIMENTO, T. C. AND SCHREINER, C. E. Adaptation and recovery from adaptation in single nerve fiber responses of the cat auditory nerve. *J. Acoust. Soc. Am.* 90: 263–273, 1991.
- FAURE, P. A. AND BARCLAY, R.M.R. The sensory basis of prey detection by the long-eared bat, *Myotis evotis*, and the consequences of prey selection. *Anim. Behav.* 44: 31–39, 1992.
- FELLEMAN, D. J. AND KAAS, J. H. Receptive-field properties of neurons in middle temporal visual area (MT) of owl monkeys. *J. Neurophysiol.* 52: 488–513, 1984.
- FENG, A. S., LIN, W.-Y., AND SUN, L. Detection of gaps in sinusoids by frog auditory nerve fibers: importance in AM coding. *J. Comp. Physiol.* [A] 175: 531–546, 1994.

- FLYNN, W. E. AND ELLIOT, D. N. Role of the pinnae in hearing. *J. Acoust. Soc. Am.* 38: 104–105, 1965.
- FUZESSERY, Z. M., BUTTENHOFF, P., ANDREWS, B., AND KENNEDY, J. M. Passive sound localization of prey by the pallid bat (*Antrozous pallidus*). *J. Comp. Physiol. [A]* 171: 767–777, 1993.
- FUZESSERY, Z. M., HARTLEY, D. J., AND WENSTRUP, J. J. Spatial processing within the mustache bat echolocation system: possible mechanisms for optimization. *J. Comp. Physiol. [A]* 170: 57–71, 1992.
- FUZESSERY, Z. M. AND POLLAK, G. D. Determinants of sound location selectivity in bat inferior colliculus: a combined dichotic and free-field stimulation study. *J. Neurophysiol.* 54: 59–83, 1985.
- FUZESSERY, Z. M., WENSTRUP, J. J., AND POLLAK, G. D. Determinants of horizontal sound location selectivity of binaurally excited neurons in an isofrequency region of the mustache bat inferior colliculus. *J. Neurophysiol.* 63: 1128–1147, 1990.
- GOLDBERG, J. M. AND BROWN, P. B. Functional organization of the dog superior olivary complex: an anatomical and electrophysiological study. *J. Neurophysiol.* 31: 639–656, 1968.
- GOOLER, D. M., CONDON, C. J., XU, J. S., AND FENG, A. S. Sound direction influences the frequency-tuning characteristics of neurons in the frog inferior colliculus. *J. Neurophysiol.* 69: 1018–1030, 1993.
- GOOLER, D. M. AND O'NEILL, W. E. Topographic representation of vocal frequency demonstrated by microstimulation of anterior cingulate cortex in the echolocating bat *Pteronotus parnellii parnellii*. *J. Comp. Physiol. [A]* 161: 283–294, 1987.
- GORDON, B. Receptive fields in deep layers of cat superior colliculus. *J. Neurophysiol.* 36: 157–178, 1973.
- GRIFFIN, D. R. *Listening in the Dark*. New Haven, CT: Yale University Press, 1958.
- GRIFFIN, D. R., WEBSTER, F. A., AND MICHAEL, C. R. The echolocation of flying insects by bats. *Anim. Behav.* 8: 141–151, 1960.
- GRINNELL, A. D. Comparative auditory neurophysiology of neotropical bats employing different echolocation signals. *Z. Vgl. Physiol.* 68: 117–153, 1970.
- HARRIS, D. M. AND DALLOS, P. Forward masking of auditory nerve fiber responses. *J. Neurophysiol.* 42: 1083–1107, 1979.
- HENSON, M. M. Unusual nerve-fibre distribution in the cochlea of the bat *Pteronotus parnellii* (Gray). *J. Acoust. Soc. Am.* 53: 1739–1740, 1973.
- HUBEL, D. H. AND WIESEL, T. N. Receptive fields, binocular interaction and functional architecture in the cat's visual cortex. *J. Physiol. (Lond.)* 160: 106–154, 1962.
- HUTSON, K. A. AND KIEBER, M. L. Ascending projections to inferior colliculus in the megachiropteran Egyptian fruit bat (*Rousettus aegyptiacus*). *Abstr. Assoc. Res. Otolaryngol.* 20: 755, 1997.
- IRVINE, D.R.F. Physiology of the auditory brainstem. In: *The Mammalian Auditory Pathway: Neurophysiology*, edited by A. N. Popper and R. R. Fay. New York: Springer-Verlag, 1992, p. 153–231.
- JEFFRESS, L. A. A place theory of sound localization. *J. Comp. Psychol.* 41: 35–39, 1948.
- JORIS, P. X. AND YIN, T.C.T. Envelope coding in the lateral superior olive. I. Sensitivity to interaural time differences. *J. Neurophysiol.* 73: 1043–1062, 1995.
- KANWAL, J. S., MATSUMURA, S., OHLEMILLER, K., AND SUGA, N. Analysis of acoustic elements and syntax in communication sounds emitted by mustached bats. *J. Acoust. Soc. Am.* 96: 1229–54, 1994.
- KIANG, N.Y.-S., WANTANABE, T., THOMAS, E. C., AND CLARK, L. F. Discharge patterns of single nerve fibers in the cat's auditory nerve. Research Monograph, No. 35, Cambridge, MA: MIT Press, 1965.
- KLEISER, A. AND SCHULLER, G. Responses of collicular neurons to acoustic motion in the horseshoe bat *Rhinolophus rouxi*. *Naturwiss.* 82: 337–340, 1995.
- KNUDSEN, E. I., DU LAC, S., AND ESTERLY, S. D. Computational maps in the brain. *Annu. Rev. Neurosci.* 10: 41–65, 1987.
- KÖSSL, M. AND VATER, M. Evoked acoustic emissions and cochlear microphonics in the mustache bat, *Pteronotus parnellii*. *Hear. Res.* 19: 157–170, 1985.
- LEE, D. N., VAN DER WEEL, F. R., HITCHCOCK, T., MATEJOWSKY, E., AND PETTIGREW, J. D. Common principle of guidance by echolocation and vision. *J. Comp. Physiol. [A]* 171: 563–571, 1992.
- MAKOUS, J. C. AND O'NEILL, W. E. Directional sensitivity of the auditory midbrain in the mustached bat to free-field tones. *Hear. Res.* 24: 73–88, 1986.
- MAUNSELL, J.H.R. AND VAN ESSEN, D. C. Functional properties of neurons in middle temporal visual area of the macaque monkey. I. Selectivity for stimulus direction, speed and orientation. *J. Neurophysiol.* 49: 1127–1147, 1983.
- MESULAM, M. M. *Tracing Neural Connections with Horseradish Peroxidase*. New York: John Wiley, 1982.
- MIDDLEBROOKS, J. C. AND GREEN, D. M. Sound localization by human listeners. *Annu. Rev. Psychol.* 42: 135–159, 1991.
- MIKAMI, A., NEWSOME, W. T., AND WURTZ, R. H. Motion selectivity in macaque visual cortex. I. Mechanisms of direction and speed selectivity in extrastriate area MT. *J. Neurophysiol.* 55: 1308–1327, 1986.
- MITTMANN, D. H. AND WENSTRUP, J. J. Combination-sensitive neurons in the inferior colliculus. *Hear. Res.* 90: 185–91, 1995.
- MØLLER, A. R. Latency of unit responses in cochlear nucleus determined in two different ways. *J. Neurophysiol.* 38: 812–821, 1975.
- MORRELL, F. Visual system's view of acoustic space. *Nature* 238: 44–46, 1972.
- MUSICANT, A. D., CHAN, J.C.K., AND HIND, J. E. Direction-dependent spectral properties of cat external ear: new data and cross-species comparisons. *J. Acoust. Soc. Am.* 87: 757–781, 1990.
- NOVICK, A. Orientation in neotropical bats. II. Phyllostomatidae and desmodontidae. *J. Mammal.* 44: 44–56, 1963a.
- NOVICK, A. Pulse duration in the echolocation of insects by the bat, *Pteronotus*. *Ergeb. Biol.* 26: 21–26, 1963b.
- NOVICK, A. AND VAISNYS, J. R. Echolocation of flying insects by the bat *Chilonycteris parnellii*. *Biol. Bull.* 127: 478–488, 1964.
- OLSEN, J. F. AND SUGA, N. Combination-sensitive neurons in the medial geniculate body of the mustached bat: encoding of target range information. *J. Neurophysiol.* 65: 1275–96, 1991.
- O'NEILL, W. E. Responses to pure tones and linear FM components of the CF-FM biosonar signal by single units in the inferior colliculus of the mustached bat. *J. Comp. Physiol. [A]* 157: 797–815, 1985.
- O'NEILL, W. E., FRISINA, R. D., AND GOOLER, D. M. Functional organization of mustached bat inferior colliculus. I. Representation of FM frequency bands important for target ranging revealed by (14) C-2-deoxyglucose autoradiography and single unit mapping. *J. Comp. Neurol.* 284: 60–84, 1989.
- O'NEILL, W. E. AND SUGA, N. Encoding of target range and its representation in the auditory cortex of the mustached bat. *J. Neurosci.* 2: 17–31, 1982.
- PERROTT, D. R. AND MUSICANT, A. D. Minimum auditory movement angle: binaural localization of moving sources. *J. Acoust. Soc. Am.* 62: 1463–1466, 1977.
- PERROTT, D. R. AND MUSICANT, A. D. Dynamic minimum audible angle: binaural spatial acuity with moving sound sources. *J. Aud. Res.* 21: 287–295, 1981.
- PHILLIPS, D. P., MENDELSON, J. R., CYNADER, M. S., AND DOUGLAS, R. M. Responses of single neurons in cat auditory cortex to time-varying stimuli: frequency-modulated tones of narrow excursion. *Exp. Brain Res.* 58: 443–454, 1985.
- POLLAK, G. D. AND BODENHAMER, R. D. Specialized characteristics of single units in inferior colliculus of mustache bat: frequency representation, tuning, and discharge patterns. *J. Neurophysiol.* 46: 605–620, 1981.
- POLLAK, G. D., HENSON, O. W., AND NOVICK, A. Cochlear microphonic audiograms in the pure tone bat *Chilonycteris parnellii parnellii*. *Science* 176: 66–68, 1972.
- POLLAK, G. D., WINER, J. A., AND O'NEILL, W. E. Perspectives on the functional organization of the mammalian auditory system: why bats are good models. In: *Hearing by Bats*, edited by A. N. Popper and R. R. Fay. New York: Springer-Verlag, 1995, p. 481–498.
- RAUSCHHECKER, J. P. AND HARRIS, L. R. Auditory and visual neurons in the cat's superior colliculus selective for the direction of apparent motion stimuli. *Brain Res.* 490: 56–63, 1989.
- ROSS, L. S., POLLAK, G. D., AND ZOOK, J. M. Origin of ascending projections to an isofrequency region of the mustache bat's inferior colliculus. *J. Comp. Neurol.* 270: 488–505, 1988.
- SCHLEGEL, P. A. Single brain stem unit responses to binaural stimuli simulating moving sounds in *Rhinolophus ferrumequinum*. In: *Animal Sonar Systems*, edited by R. G. Busnel and I. F. Fish. New York: Plenum Press, 1980, p. 973–975.
- SCHULLER, G., RADTKE-SCHULLER, S., AND BETZ, M. A stereotaxic method for small animals using experimentally determined reference profiles. *J. Neurosci. Methods* 18: 339–350, 1986.
- SIMMONS, J. A., KICK, S. A., LAWRENCE, B. D., HALE, C., BARD, C., AND ESCUDIE, B. Acuity of horizontal angle discrimination by the echolocating bat *Eptesicus fuscus*. *J. Comp. Physiol. [A]* 153: 321–330, 1983.

- SOKAL R. R. AND ROHLF, F. J. *Biometry: The Principles and Practice of Statistics in Biological Research* (2nd ed.). New York: W. H. Freeman, 1981.
- SOVIJÄRVI, A.R.A. AND HYVÄRINEN, J. Auditory cortical neurons in the cat sensitive to the direction of sound source movement. *Brain Res.* 73: 455–471, 1974.
- SPITZER, M. W. AND SEMPLE, M. N. Interaural phase coding in auditory midbrain: influence of dynamic stimulus features. *Science* 254: 721–724, 1991.
- SPITZER, M. W. AND SEMPLE, M. N. Responses of inferior colliculus neurons to time-varying interaural phase disparity: effects of shifting the locus of virtual motion. *J. Neurophysiol.* 69: 1245–1263, 1993.
- STRYBEL, T. Z., MANLIGAS, C. L., AND PERROTT, D. R. Auditory apparent motion under binaural and monaural listening conditions. *Percept. Psychophys.* 45: 371–377, 1989.
- STRYBEL, T. Z., WITTY, A. M., AND PERROTT, D. R. Auditory apparent motion in the free field: the effects of stimulus duration and separation. *Percept. Psychophys.* 52: 139–143, 1992.
- STUMPF, E., TORONCHUK, J. M., AND CYNADER, M. S. Neurons in cat primary cortex sensitive to correlates of auditory motion in three-dimensional space. *Exp. Brain Res.* 88: 158–68, 1992.
- SUZUKI, D. A., MAY, J. G., KELLER, E. L., AND YEE, R. D. Visual motion response properties in dorsolateral pontine nucleus of alert monkey. *J. Neurophysiol.* 63: 37–59, 1990.
- SUGA, N. Cortical computational maps for auditory imaging. *Neural Networks* 3: 3–21, 1990.
- SUGA, N. AND JEN, P. H. Disproportionate tonotopic representation for processing CF-FM sonar signals in the mustache bat auditory cortex. *Science* 194: 542–544, 1976.
- SUGA, N. AND MANABE, T. Neural basis of amplitude-spectrum representation in auditory cortex of the mustached bat. *J. Neurophysiol.* 47: 225–255, 1982.
- SUGA, N. AND O'NEILL, W. E. Neural axis representing target range in the auditory cortex of the mustache bat. *Science* 206: 351–3, 1979.
- SUGA, N., SIMMONS, J. A., AND JEN, P. H. Peripheral specialization for fine analysis of Doppler-shifted echoes in the auditory system of the "CF-FM" bat. *Pteronotus parnellii*. *J. Exp. Biol.* 63: 161–192, 1975.
- TAKAHASHI, T. T. AND KELLER, C. H. Simulated motion enhances neural sensitivity for a sound localization cue in background noise. *J. Neurosci.* 12: 4381–4390, 1992.
- TORONCHUK, J. M., STUMPF, E., AND CYNADER, M. S. Auditory cortex neurons sensitive to correlates of auditory motion: underlying mechanisms. *Exp. Brain Res.* 88: 169–180, 1992.
- VAN ESSEN, D. C. AND MAUNSELL, J.H.R. Hierarchical organization and functional streams in the visual cortex. *Trends Neurosci.* 8: 370–375, 1983.
- WAGNER, H. AND TAKAHASHI, T. Neurons in the midbrain of the barn owl are sensitive to the direction of apparent acoustic motion. *Naturwissenschaften* 77: 439–442, 1990.
- WAGNER, H. AND TAKAHASHI, T. Influence of temporal cues on acoustic motion-direction sensitivity of auditory neurons in the owl. *J. Neurophysiol.* 68: 2063–2076, 1992.
- WENSTRUP, J. J., FUZESEY, Z. M., AND POLLAK, G. D. Binaural interactions in the mustache bat's inferior colliculus. II. Determinants of spatial responses among 60-kHz EI units. *J. Neurophysiol.* 60: 1384–1404, 1988.
- WENSTRUP, J. J., ROSS, L. S., AND POLLAK, G. D. Binaural response organization within a frequency-band representation of the inferior colliculus: implications for sound localization. *J. Neurosci.* 6: 962–973, 1986.
- WICKELGREN, B. G. Superior colliculus: some receptive field properties of bimodally responsive cells. *Science* 173: 69–72, 1971.
- WILSON W. W. AND O'NEILL, W. E. Single-unit responses in bat auditory midbrain to dichotic and free-field correlates of auditory motion: direction dependent shifts in response properties. *Abstr. Assoc. Res. Otolaryngol.* 18: 257, 1995.
- YAN, J. AND SUGA, N. The midbrain creates and the thalamus sharpens echo-delay tuning for the cortical representation of target-distance information in the mustached bat. *Hear. Res.* 93: 102–110, 1996.
- YIN, T. C. AND KUWADA, S. Binaural interaction in low-frequency neurons in the inferior colliculus of the cat. III. Effects of changing frequency. *J. Neurophysiol.* 50: 1020–1042, 1983.
- YIN, T. C., KUWADA S., AND SUJAKU Y. Interaural time sensitivity of high-frequency neurons in the inferior colliculus. *J. Acoust. Soc. Am.* 76: 1401–1410, 1984.
- ZOOK, J. M. AND CASSEDAY, J. H. Cytoarchitecture of auditory system in lower brainstem of the mustache bat. *Pteronotus parnellii*. *J. Comp. Neurol.* 207: 1–13, 1982a.
- ZOOK, J. M. AND CASSEDAY, J. H. Origin of ascending projections to the inferior colliculus in the mustache bat. *Pteronotus parnellii*. *J. Comp. Neurol.* 207: 14–28, 1982b.
- ZOOK, J. M., WINER, J. A., POLLAK, G. D., AND BODENHAMER, R. D. Topology of the central nucleus of the mustache bat's inferior colliculus: correlation of single unit properties and neuronal architecture. *J. Comp. Neurol.* 231: 530–546, 1985.